

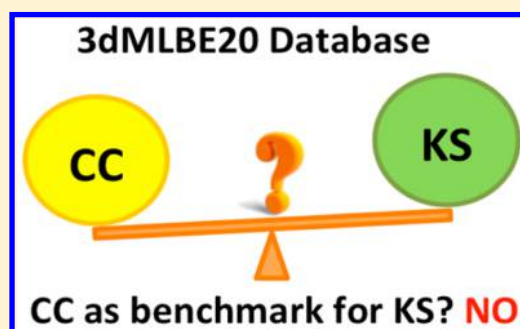
Do Practical Standard Coupled Cluster Calculations Agree Better than Kohn–Sham Calculations with Currently Available Functionals When Compared to the Best Available Experimental Data for Dissociation Energies of Bonds to 3d Transition Metals?

Xuefei Xu,[†] Wenjing Zhang,^{†,‡} Mingsheng Tang,[‡] and Donald G. Truhlar^{*,†}

[†]Department of Chemistry, Chemical Theory Center, and Supercomputing Institute, University of Minnesota, Minneapolis, Minnesota 55455-0431, United States

[‡]College of Chemistry and Molecular Engineering, Zhengzhou University, Zhengzhou, Henan Province 450001, People's Republic of China

ABSTRACT: Coupled-cluster (CC) methods have been extensively used as the high-level approach in quantum electronic structure theory to predict various properties of molecules when experimental results are unavailable. It is often assumed that CC methods, if they include at least up to connected-triple-excitation quasiperturbative corrections to a full treatment of single and double excitations (in particular, CCSD(T)), and a very large basis set, are more accurate than Kohn–Sham (KS) density functional theory (DFT). In the present work, we tested and compared the performance of standard CC and KS methods on bond energy calculations of 20 3d transition metal-containing diatomic molecules against the most reliable experimental data available, as collected in a database called 3dMLBE20. It is found that, although the CCSD(T) and higher levels CC methods have mean unsigned deviations from experiment that are smaller than most exchange–correlation functionals for metal–ligand bond energies of transition metals, the improvement is less than one standard deviation of the mean unsigned deviation. Furthermore, on average, almost half of the 42 exchange–correlation functionals that we tested are closer to experiment than CCSD(T) with the same extended basis set for the same molecule. The results show that, when both relativistic and core–valence correlation effects are considered, even the very high-level (expensive) CC method with single, double, triple, and perturbative quadruple cluster operators, namely, CCSDT(2)_Q, averaged over 20 bond energies, gives a mean unsigned deviation (MUD(20) = 4.7 kcal/mol when one correlates only valence, 3p, and 3s electrons of transition metals and only valence electrons of ligands, or 4.6 kcal/mol when one correlates all core electrons except for 1s shells of transition metals, S, and Cl); and that is similar to some good xc functionals (e.g., B97-1 (MUD(20) = 4.5 kcal/mol) and PW6B95 (MUD(20) = 4.9 kcal/mol)) when the same basis set is used. We found that, for both coupled cluster calculations and KS calculations, the *T*₁ diagnostics correlate the errors better than either the *M* diagnostics or the *B*₁ DFT-based diagnostics. The potential use of practical standard CC methods as a benchmark theory is further confounded by the finding that CC and DFT methods usually have different signs of the error. We conclude that the available experimental data do not provide a justification for using conventional single-reference CC theory calculations to validate or test xc functionals for systems involving 3d transition metals.



1. INTRODUCTION

Transition-metal compounds are very important for many applications, including materials synthesis, photochemistry, and industrial and biological catalysis. An area of rapid growth and great future promise is the computational design of new catalytic systems, for example, metal–organic frameworks, involving Earth-abundant 3d transition metals. The first step toward understanding many catalyzed and uncatalyzed reactions is to consider the energy of reactants, products, and intermediates, such as catalyst–substrate complexes, and the barrier of reaction, which are closely related to the energies of broken and formed bonds in the reaction; however, in many complexes involving metal atoms, the experimental bond energies have large uncertainties or are even unavailable. In such cases, one might

turn to quantum mechanical electronic structure methods, such as coupled cluster (CC) wave function theory or Kohn–Sham (KS) density functional theory (DFT). Therefore, it is very important to understand the quantitative reliability (or unreliability) of these methods for predicting the bond energies of transition-metal-containing systems.

CC theory¹ is usually considered to be the most accurate and most powerful electronic structure method that is applicable to moderate-sized molecules, and it has been successfully applied for the prediction and in-depth understanding of chemical structure, properties, reactivity, and mechanisms. CC theory

Received: November 29, 2014

Published: March 19, 2015

becomes exact as one includes successively higher and higher excitation operators (double, triple, quadruple, ...), but for many complex systems, CC calculations are not affordable (although recent advances are changing this situation dramatically²), and even when such calculations are affordable, one is often limited to double excitations with a quasi-perturbative treatment of connected triple excitations. However, this theory, called CCSD(T),³ is very successful and has even been called the “gold standard” of quantum chemistry.⁴

The trust in CCSD(T) calculations is so high that, in the absence of experimental data, CCSD(T) results are frequently used as reference values (also called benchmark values) of chemical properties; for example, CCSD(T) calculations are often used for validation of the accuracy of other theoretical methods, such as KS methods.⁵ One must be cautious, however, for a couple of reasons. First of all, CCSD(T) is very slowly convergent, with respect to the completeness of the one-electron basis set. Although this convergence can be accelerated with explicitly correlated basis functions,⁶ and although extrapolation to the complete basis set limit is reasonably accurate if one can afford calculations with sufficiently large basis sets as input to the extrapolation, these procedures still increase the cost enormously. This can be especially troublesome for calculations involving atoms from the fourth period and beyond (K or heavier), where it may be necessary to use not only a large valence basis set but also basis functions capable of representing core–valence correlation. A second concern is that the CCSD(T) method is a single-reference method, and its reliability is questionable for intrinsically multiconfigurational systems, usually called multireference (MR) systems and sometimes described as systems with high static correlation; most generally, MR systems are those for which more than one configuration state function has a moderate or large contribution to the wave function of system. A majority of the validation studies on which the confidence in CCSD(T) rests are for single-reference systems, where the wave function has only small contributions from other than the leading configuration state function, although there is some important work testing the theory for multireference systems.^{7,8} Nevertheless, the question arises of whether (and when) one must use multireference methods, such as multireference configuration interaction (MRCI) and complete active space second perturbation theory (CASPT2),⁹ or some advanced CC methods¹⁰ stimulated by the multireference problem, as the source of benchmark data for multireference systems.

Both the above sources of concern are prominent for applications to catalysis. First, reliable extrapolation to the CBS limit is often unaffordable for real catalysts, and one must know how reliable are calculations with affordable basis sets such as multiply polarized triple- ζ sets, with or without diffuse function augmentation and with or without core–valence basis functions. Second, the electronic structure of transition-metal-containing catalytic intermediates often has multireference character, because of open d subshells.¹¹ In many cases, practical limitations mean that KS theory is used without system-specific validation. Therefore, validation of both conventional CC theory and KS theory against standard reference suites can be very useful.

KS theory is, in principle, exact for all systems, even for multireference systems, if one uses the exact exchange–correlation (xc) functional.¹² But, unfortunately, the exact functional is essentially unknowable,¹³ so the accuracy of an xc functional is dependent on the quality of the approximation to the xc functional. It has been found that many problems involving

only main-group nonmetal elements can be treated with reasonably high accuracy, especially with functionals^{14,15} developed in the past decade. Many validation suites have also been carried out for KS theory applied to transition-metal systems.¹⁶ A finding of such studies is that many presently available xc functionals show significantly larger errors in calculating chemical energies of systems containing transition-metal atoms. This failure is generally attributed to the multireference characters shown by the transition metals, although we have recently found that the actual situation may be more complicated.¹⁷ For example, we have found that molecules containing main-group metals are also more difficult for KS theory with existing functionals than are molecules containing only main-group nonmetal elements.

For main-group chemistry involving mainly single-reference systems, the effect of higher excitations (full treatment of connected triple excitations and quasiperturbative inclusion of connected quadruple or higher excitations) has been well-studied, and CC theory with a high level of excitations has been found to have very high accuracy for some small molecules, but there is less work on such studies for transition metals. This is an example of a more general issue, namely that consistent tests of CC theory and KS theory *on the same set of data* are scarce. The main objective of the present work is to provide such a consistent set of tests. We can keep in mind that CC theory would be exact if we used all the higher-order excitations and a complete basis set, and KS theory would be exact if we used the exact functional and a complete basis set. But both of these options are impractical, even impossible, so the best that we can do is to compare practical versions of CC theory with KS theory using the best available functionals, both with reasonable (but incomplete) basis sets.

In one recent work by three of the present authors,¹⁸ we tested the performance of 42 xc functionals^{14,15,19–49} for predicting the average bond energies of 70 3d transition-metal-containing compounds (the 3dBE70 database) against reliable experimental data. Since Wilson and co-workers have noted that, for the subset of molecules where the experiments are less uncertain, the performance of coupled cluster theory improves significantly, that study¹⁸ was based on only data for molecules in the group where Wilson and co-workers said the experimental error is smallest. (The present study is then based on a subset of that carefully chosen set of data.) Ten (10) of the 42 xc functionals were found¹⁸ to have a mean unsigned deviation (MUD) over 70 molecules smaller than 4.0 kcal/mol. One question raised by that study is that how well CCSD(T) or even higher-level CC methods, such as CCSDT⁵⁰ which fully includes all connected single, double, and triple excitations, and CCSDT(2)_Q⁵¹ with a second-order quadruples correction to full single, double, and triple excitations, can perform if tested consistently on the same set of transition-metal–ligand bonds. Are CC methods, which are close to limit of practicality, good enough to be benchmarks to validate KS functionals for this type of system? Although the CCSD(T) method has been found to be problematic for calculations of transition-metal-containing compounds,⁵² to the best of our knowledge, systematic research on the relative performance of coupled-cluster methods and approximate density functionals on bond energy calculations involving transition metals has not been reported. In the present paper, we will construct a new database including 20 bond energies of 3d transition-metal-containing diatomic molecules (denoted as 3dMLBE20, where MLBE denotes “metal–ligand bond energies”), to test the performances of CC methods (CCSD,

Table 1. 3dMLBE20 Database: Ground Electronic States of Molecules and Atoms, Best Estimated Bond Lengths (r_e), Reference Equilibrium Bond Dissociation Energies (D_e) and Uncertainties of D_e , and Spin-Orbit Energies (E_{SO})

molecule	state	r_e (Å)	D_e (kcal/mol)	uncertainty (kcal/mol)	E_{SO}^a (kcal/mol)	atom	state	E_{SO}^b (kcal/mol)
TiCl	$^4\Phi$	2.265 ^c	100.8 ^d	2.0 ^d	−0.5	Ti	3F	−0.6
VH	$^5\Delta$	1.730 ^e	51.4 ^d	1.6 ^d	−0.5	V	4F	−0.9
VO	$^4\Sigma^-$	1.589 ^f	151.0 ^d	2.0 ^d	0	Cr	7S	0
VCl	$^5\Delta$	2.215 ^c	101.9 ^d	2.0 ^d	−0.4	Mn	6S	0
CrH	$^6\Sigma^+$	1.656 ^f	46.8 ^d	1.6 ^d	0	Fe	5D	−1.2
CrO	$^5\Pi$	1.621 ^f	104.7 ^g	1.2 ^g	−0.4	Co	4F	−2.3
CrCl	$^6\Sigma^+$	2.194 ^c	90.1 ^d	1.6 ^d	0	Ni	3F	−2.8
MnS	$^6\Sigma^+$	2.070 ^e	70.5 ^d	2.0 ^d	0	Cu	2S	0
MnCl	$^7\Sigma^+$	2.243 ^h	80.7 ^d	1.6 ^d	0	Zn	1S	0
FeH	$^4\Delta$	1.630 ^e	36.9 ^g	0.8 ^g	−1.1	H	2S	0
FeCl	$^6\Delta$	2.179 ⁱ	78.5 ^d	1.6 ^d	−1.1	O	3P	−0.2
CoH	$^3\Phi$	1.530 ^e	45.5 ^g	1.2 ^g	−2.1	S	3P	−0.6
CoCl	$^3\Phi$	2.087 ^h	80.5 ^d	1.6 ^d	−2.1	Cl	2P	−0.8
NiCl	$^2\Pi$	2.073 ^h	88.0 ^d	1.0 ^d	−1.5			
CuH	$^1\Sigma^+$	1.463 ^f	62.6 ^g	1.4 ^g	0			
CuCl	$^1\Sigma$	2.050 ^e	87.7 ^d	0.4 ^d	0			
ZnH	$^2\Sigma^+$	1.590 ^e	21.6 ^d	0.5 ^d	0			
ZnO	$^1\Sigma$	1.800 ^e	37.9 ^d	0.9 ^d	0			
ZnS	$^1\Sigma$	2.100 ^e	34.3 ^d	1.0 ^d	0			
ZnCl	$^2\Sigma$	2.100 ^e	53.5 ^d	1.0 ^d	0			

^aThe spin–orbit energies of molecules which have a non- Σ ground state are estimated at the CASSCF level, and in particular, the active space used in calculations is TiCl, CAS(5,9); VH, CAS(6,8); VCl, CAS(6,9); CrO, CAS(6,9); FeH, CAS(9,8); FeCl, CAS(9,9); CoH, CAS(10,8); CoCl, CAS(10,9); NiCl, CAS(11,9). ^bThe atomic spin–orbit energies are from refs 7, 80, and 81. ^cData taken from ref 82. ^dObtained in the same way as in ref 18. Note that, here, D_e includes the spin–orbit effect. The uncertainty is that in the heat of formation. ^eData taken from ref 83. ^fData taken from ref 84. ^g $D_e = D_0 + E_{ZPE}$, D_0 and uncertainty are from ref 54; zero point energy E_{ZPE} is obtained by M06-L/ma(L)-TZVP with a scaling factor of 0.976. ^hOptimized by M06-L/ma(L)-TZVP. ⁱData taken from ref 85.

CCSD(T), CCSDT, and CCSDT(2)_Q) and compare this performance consistently to that of KS methods. For comparison, we also tested the performance of second-order Møller–Plesset perturbation theory (MP2).⁵³ We note that quadruple excitations are usually impractical for complex systems, but by limiting ourselves here to diatomic molecules, we can afford them. In fact, even triple excitations and sometimes even double excitations are often unaffordable for complex systems.

2. DATABASE 3dMLBE20

The 3dBE70 database was originally selected from an even larger database⁷ as consisting of the molecules with the most reliable experimental data. The 20 molecules in the 3dMLBE20 database consist of 19 diatomic metal–ligand molecules in the 3dBE70 database¹⁸ plus the CoH molecule selected from a previously reported database called SRMBE13.⁴⁷ The new test suite is limited to diatomic molecules so that very-high-level CC calculations are possible. The CoH molecule is included because (i) we found that most of the xc functionals tested in ref 18 perform systematically worse for its bond energy than for those of other molecules and (ii) CoH has very large multireference character (as will be detailed below).

Table 1 lists all the molecules included in the 3dMLBE20 database, the term symbols of the ground electronic states of these molecules and their constituent atoms, the corresponding best estimated bond lengths to be used in the present work, and the reference experimental equilibrium bond dissociation energies D_e and their stated uncertainties. Except for CrO, FeH, CoH, and CuH, the reference D_e values and their uncertainties in Table 1 were obtained from the experimental

enthalpy of formation,⁷ with vibrational corrections calculated at the M06-L/ma(L)-TZVP in the same way as explained in ref 18.

For CrO, FeH, CoH, and CuH, because more direct and accurate experimental dissociation energies at 0 K (D_0) are available,⁵⁴ the D_e values were obtained directly by adding the zero-point-energy corrections calculated by M06-L/ma(L)-TZVP with a vibrational-frequency scaling factor of 0.976 to D_0 . The M06-L density functional was selected for this purpose, because of its good performance for geometry optimization. The ma(L)-TZVP basis is defined as follows: it consists of the def2-TZVP⁵⁵ basis set for metal elements and hydrogen atoms and the minimally augmented def2-TZVP basis set (ma-TZVP)⁵⁶ for nonmetal, nonhydrogenic ligands L (in the present work, L = H, O, S, or Cl).

For the purpose of understanding the performance of CC and KS methods better, the 3dMLBE20 database is further divided to two subsets, based on the extent of multireference character of the molecular wave functions: a single reference database called 3dMLBE-SR7 with 7 molecules (MnCl, ZnCl, FeCl, CrCl, ZnS, ZnH, and CuCl) with less multireference character, and a multireference database called 3dMLBE-MR13 including the other 13 molecules with larger multireference character. Three multireference diagnostics are used to divide the database: (i) the T_1 diagnostic^{57,58} calculated by CCSD/ma(L)-TZVP//ref, (ii) the M diagnostic⁵⁹ calculated by CASSCF^{60,61}/ma(L)-TZVP//ref, and (iii) the B_1 diagnostic⁶² calculated by BLYP/ma(L)-TZVP and B1LYP/ma(L)-TZVP//BLYP/ma(L)-TZVP. The notation “//ref” denotes that the reference bond lengths given in Table 1 are used in the calculations. We next give some background on the three diagnostics.

The T_1 diagnostic is the oldest.⁵⁷ It is a measure of the contribution of single excitations to the CCSD amplitude. Since single excitations have the largest effect on the electron density, and since the Hartree–Fock reference state of the CCSD method has no first-order correction to the density, it is thought that a larger-than-usual density correction is a signal of higher-than-usual errors in the single-configuration reference function. The border between small and moderate is not precise but is usually assumed to be located between about 0.02 and 0.04.

The B_1 diagnostic⁶² is the difference in bond energy calculated by two KS calculations whose only difference is the substitution of 25% Hartree–Fock exchange for B88 local exchange in a generalized gradient approximation. Since Hartree–Fock exchange brings about a static correlation error,⁶³ a large change in bond energy due to this substitution could be a mark of multireference character. However, it could also have other causes, for example, the poor performance of the B88 exchange functional. The border between small and large multireference character was originally estimated to be ~ 10 kcal/mol. Recently, Martin and co-workers⁶⁴ proposed a very similar density functional diagnostic and concluded, based on tests involving systems containing only main-group elements, that it is very useful, so further testing of this type of functional is worthwhile. The B_1 diagnostic is calculated by

$$B_1 = D_e^{\text{BLYP}} - D_e^{\text{BLYP//BLYP}} \quad (1)$$

In eq 1, D_e^{BLYP} is the bond dissociation energy calculated by BLYP/ma(L)-TZVP with the optimized geometry at the same level, and $D_e^{\text{BLYP//BLYP}}$ is the bond dissociation energy calculated by BLYP/ma(L)-TZVP at a geometry optimized at the BLYP/ma(L)-TZVP level.

The M diagnostic⁵⁹ seems to be the best founded of the three. It is a measure of the deviation of the HOMO natural orbital occupancy from 2, the SOMO natural orbital occupancy or occupancies (if any single occupied orbitals are present) from one, and the LUMO natural orbital occupancies from zero. It was originally proposed that $M < 0.05$ indicates small multireference character, an M value between 0.05 and 0.1 implies moderate multireference character, and $M > 0.1$ implies high multireference character. In their recent comparison of multireference diagnostics, Martin and co-workers⁶⁴ used very expensive wave function diagnostics and showed that one could also make a good, inexpensive diagnostic with density functional theory (DFT), as mentioned in the previous paragraph, and they also studied less expensive wave function diagnostics, such as the T_1 and M diagnostics. They concluded that, “Of the wave function-based diagnostics, the only one that has a reasonable correlation with [a very expensive benchmark diagnostic] is Truhlar’s M diag”. The M diagnostic is given by

$$M = \frac{1}{2} \left(2 - n(\text{MCDONO}) + n(\text{MCUNO}) + \sum_{j=1}^{n_{\text{SOMO}}} \ln(j) - 1 \right) \quad (2)$$

where $n(\text{MCDONO})$ stands for the smallest natural orbital occupation number of the “doubly occupied” (that refers to the dominant configuration) natural orbitals, $n(\text{MCUNO})$ for the largest natural orbital occupation number of the “unoccupied” (again, in the dominant configuration) natural orbitals, $n(j)$ stands for the natural orbital occupation number of singly

occupied natural orbital j , and n_{SOMO} is the number of singly occupied molecular orbitals in the dominant configuration of the ground electronic state. The CASSCF calculations were carried out within C_{2v} symmetry using the Molpro 2010.1⁶⁵ package, and the active space consisted of the $4s3d$ orbitals of transition metals, the $3s3p_z4s$ orbitals of S and Cl, the $2s2p_z3s$ orbitals of O, and the $1s2s$ orbitals of H and the corresponding electrons were included in the active space.

The analysis and discussion of the multireference character of the molecules in our database is given later in section 7.3.

3. ELECTRONIC STRUCTURE COMPUTATIONAL DETAILS

In KS or CC calculations, the equilibrium bond dissociation energy D_e of diatom XY is calculated (calc) by

$$D_e(\text{calc}) = E(X) + E_{\text{SO}}(X) + E(Y) + E_{\text{SO}}(Y) - E(XY) - E_{\text{SO}}(XY) \quad (3)$$

where $E(Z)$ is the energy of species Z ($Z = X, Y$, or XY) calculated (by CC theory, KS theory, or MP2 theory) without including spin–orbit coupling, and $E_{\text{SO}}(Z)$ is our best estimate of the spin–orbit energy, which is always negative or zero. For atoms, $E_{\text{SO}}(Z)$ is easily calculated from well-known atomic energy levels, and, here, we use standard values from the literature. For linear molecules with a Σ ground state, the spin–orbit energy is zero by symmetry. For other molecules, spin–orbit energies were calculated. In these calculations, the spin–orbit matrix elements were estimated by the state-averaged CASSCF method with the Breit–Pauli operator using the Molpro 2010.1 package, and spin–orbit eigenstates were obtained by diagonalizing the effective spin–orbit Hamiltonian;⁶⁶ the energy lowering of the lowest spin–orbit eigenstate compared to the state-averaged ground state is taken as the spin–orbit energy. For the CASSCF calculations, we used the ma(L)-TZVP basis set (defined above) and C_{2v} symmetry, and the active space consisted of the $4s3d$ orbitals of transition metals, the $3s3p_z4s$ orbitals of Cl, the $2s2p_z3s$ orbitals of O, and the $1s2s$ orbitals of H and the corresponding electrons were included in the active space. The experimental atomic spin–orbit energies and calculated molecular spin–orbit energies are given in Table 1.

4. SELECTION OF EXCHANGE-CORRELATION FUNCTIONALS TO BE STUDIED AND THEIR MEAN ERRORS

The present work has two goals: one is testing performance of the conventional CC calculations with various excitation levels on bond energies of the $3d$ transition-metal–ligand molecules; another is comparing their performance to those of various KS xc functionals on the same set of data. Except for CoH, the molecules in database 3dMLBE20 have already been used for testing KS theory in ref 18. The first step in the present work was applying precisely the same methodologies as those described in ref 18 to calculate bond energies of CoH, using the 42 xc functionals tested in ref 18. In particular, we used a locally modified version of the Gaussian 09 program,⁶⁷ ma(L)-TZVP basis set, and pruned integration grids with 99 radial shells and 590 angular points in each shell (which is called “ultrafine” grid in Gaussian 09). The geometries (i.e., bond distances) were optimized, and all KS calculations were performed allowing symmetry to be broken by using the keyword `stable = opt` in Gaussian 09; in broken-symmetry calculations, the wave function

Table 2. Top 20 Exchange-Correlation Functionals Tested in This Work and Their Mean Signed Deviations and Mean Unsigned Deviations (MSD(20) or MUD(20) (kcal/mol)) over the 20 Bond Energies, As Compared to the Reference D_e Values in Table 1^a

xc	MSD(20)	MUD(20)	ref	xc	MSD(20)	MUD(20)	ref
B97-1	1.7	5.1	27	MPWB1K	−1.6	5.9	30
ωB97X-D	1.2	5.4	39	M08-HX	0.0	6.0	40
MPW1B95	1.6	5.5	30	B3LYP	0.1	6.1	29
PW6B95	1.4	5.5	32	PBE0	1.8	6.1	36
PW6B95-D3(BJ)	2.1	5.6	22,32	M06	−1.4	6.5	15
τ-HCTHhyb	3.4	5.7	46	M06-2X	−3.4	6.7	15
M06-D3(BJ)	−1.0	5.7	15, 22	ωB97X	0.9	6.8	45
B97-3	0.2	5.8	37	O3LYP	1.5	6.8	25
M08-SO	−0.9	5.8	40	HSE	3.0	6.9	35
M06-L	4.7	5.9	14	M05	0.6	7.1	24

^aThis table is based on calculations including spin–orbit coupling, but neglecting scalar relativistic effects (neglecting scalar relativistic effects is denoted as NDK when a short notation is needed later in the paper). It is based on consistently optimized bond lengths (i.e., bond lengths for each xc functional optimized with that functional), and the ma(L)-TZVP basis set is used for all results in this table.

Table 3. Errors (kcal/mol) Relative to the Reference D_e ^a

	//ref										
	ma(L)-TZVP	apTZ									
		ma(L)-TZVP									
	B97-1	B97-1	B97-1	B97-1	B97-1	PW6B95	PW6B95	τ -HCTHhyb	τ -HCTHhyb	M06-L	M06-L
molecule	NDK	NDK	DK	NDK	DK	NDK	DK	NDK	DK	NDK	DK
3dMLBE-SR7											
MnCl	−6.3	−6.2	−7.9	−5.3	−7.3	2.3	0.4	−7.1	−9.3	3.3	1.3
ZnCl	−4.7	−5.7	−7.4	−4.7	−7.3	−2.6	−5.5	−4.9	−7.5	−2.2	−4.7
FeCl	6.7	−1.6	−3.6	−0.7	−3.2	4.6	2.1	−1.3	−3.6	5.3	4.9
CrCl	0.7	1.2	2.0	1.9	2.2	−2.6	−2.2	3.4	3.5	8.4	8.8
ZnS	−0.3	−0.4	−1.7	0.7	−1.5	−0.7	−2.9	0.3	−1.9	1.5	−0.6
ZnH	−2.0	−2.2	−3.0	−1.6	−2.8	1.3	0.0	−0.7	−1.9	−1.6	−2.5
CuCl	−1.6	−1.8	−1.4	−0.4	−0.5	−3.1	−3.2	1.2	1.0	3.4	3.6
MUD(SR7)	3.2	2.7	3.9	2.2	3.5	2.5	2.3	2.7	4.1	3.7	3.8
3dMLBE-MR13											
ZnO	−7.8	−8.2	−9.7	−5.8	−8.0	−8.5	−10.9	−4.4	−7.9	−4.9	−6.7
NiCl	−0.3	−0.4	−1.2	0.0	−0.8	−2.9	−2.6	2.8	1.4	0.3	−3.4
TiCl	−0.3	−0.3	−2.3	0.3	−1.9	5.1	3.1	2.1	−0.2	10.1	7.3
CuH	−0.9	−1.0	1.4	0.3	2.7	−1.3	1.2	3.4	5.7	2.6	5.2
VO	−4.4	−4.6	−5.2	−3.6	−4.2	−2.1	−2.8	0.7	0.8	−0.2	0.2
VCl	−2.9	−3.0	−5.5	−2.5	−4.8	3.7	1.1	−0.4	−2.5	3.0	1.1
MnS	0.1	0.1	−2.0	0.7	−1.6	2.1	−0.1	2.6	0.1	12.1	9.8
CrO	−1.9	−2.0	1.9	−0.6	2.9	−10.1	−6.6	2.8	6.1	3.8	7.1
CoH	18.3	18.2	10.4	18.9	11.2	11.8	16.8	20.5	17.3	13.2	20.9
CoCl	12.3	12.2	2.8	13.0	3.4	7.2	7.9	14.0	8.8	10.6	2.1
VH	7.4	7.3	5.2	8.0	6.1	14.9	12.7	10.0	8.8	10.0	9.1
FeH	15.1	14.7	10.9	12.8	9.2	14.7	11.0	19.1	15.7	14.8	13.1
CrH	7.1	7.1	8.6	7.6	9.0	4.3	5.5	10.6	11.9	11.8	13.1
MUD(MR13)	6.1	6.1	5.2	5.7	5.0	6.8	6.3	7.2	6.7	7.5	7.6
3dMLBE20											
MSD(20)	1.7	1.2	−0.4	1.9	0.1	1.9	1.3	3.7	2.3	5.3	4.5
MUD(20)	5.1	4.9	4.7	4.5	4.5	5.3	4.9	5.6	5.8	6.2	6.3

^aThe values in the first column of results were calculated using the bond length optimized by B97-1/ma(L)-TZVP/NDK; for the other columns we use the reference bond length given in Table 1.

was repeatedly optimized with the appropriate reduction in constraints (if instability is detected) until the wave function is stable. In KS calculations, the basis sets employed spherical-harmonic angular functions.

We then combined the new results for CoH with the results for the 19 diatomic molecules in ref 18 to calculate the mean signed deviation [MSD(20)] and mean unsigned deviation [MUD(20)] for all 42 xc functionals on the 3dMLBE20 database. The 20 xc functionals with the smallest MUD will be

compared to CC theory in the present paper; they are listed in Table 2 with their MSD(20) and MUD(20) values.

5. SCALAR RELATIVISTIC EFFECTS AND BASIS SET EFFECTS

Vector relativistic effects (i.e., spin–orbit coupling) are considered above and are included in all calculations in this paper. For quantitative purposes, the scalar relativistic effect should also be considered for transition-metal-containing

Table 4. Scalar Relativistic Effects (kcal/mol)^a

	B97-1 ma(L)-TZVP	B97-1 apTZ	PW6B95 apTZ	τ -HCTHhyb apTZ	M06-L apTZ	CCSD(T) apTZ	CCSD(T), CV ^b apTZ
TiCl	-2.1	-2.2	-2.1	-2.3	-2.7	-1.3	-1.5
VH	-2.0	-1.8	-2.1	-1.2	-0.9	-1.6	-1.9
VO	-0.6	-0.5	-0.6	0.1	0.4	-0.6	-0.8
VCl	-2.5	-2.3	-2.6	-2.1	-1.9	-1.8	-2.1
CrH	1.5	1.4	1.2	1.3	1.3	1.6	1.5
CrO	3.9	3.5	3.5	3.2	3.2	4.0	3.8
CrCl	0.8	0.4	0.4	0.2	0.4	-0.9	-1.8
MnS	-2.0	-2.3	-2.2	-2.5	-2.3	-1.5	-1.7
MnCl	-1.6	-2.0	-2.0	-2.2	-2.0	-1.6	-1.6
FeH	-3.8	-3.6	-3.7	-3.4	-1.7	-2.8	-3.2
FeCl	-2.0	-2.5	-2.5	-2.3	-0.4	-2.1	-2.2
CoH	-7.8	-7.7	5.1	-3.3	7.6	-4.3	-4.5
CoCl	-9.3	-9.6	0.7	-5.2	-8.5	-6.4	-6.7
NiCl	-0.8	-0.8	0.3	-1.3	-3.7	-8.2	-8.4
CuH	2.4	2.4	2.5	2.3	2.6	2.6	2.6
CuCl	0.5	-0.1	0.0	-0.2	0.2	-0.1	-0.1
ZnH	-0.8	-1.2	-1.3	-1.3	-1.0	-1.4	-1.4
ZnO	-1.5	-2.2	-2.4	-3.5	-1.8	-2.6	-2.7
ZnS	-1.3	-2.1	-2.2	-2.2	-2.1	-2.1	-2.1
ZnCl	-1.7	-2.6	-2.9	-2.6	-2.5	-2.9	-2.9
MSRE(20)	-1.5	-1.8	-0.7	-1.4	-0.8	-1.7	-1.9
MURE(20)	2.5	2.6	2.0	2.1	2.4	2.4	2.6

^a//ref. ^bCV means that outer-core–valence correlation energy is included in the calculations, i.e., only 1s2s2p orbitals are frozen for 3d transition metals in the CC calculations.

systems, and an absolute average of the scalar relativistic effect over 10 small 3d transition-metal-containing systems was reported as ~2–3 kcal/mol for a few xc functionals in a previous study.⁶⁸ In the present work, to further document the effect of including scalar relativistic effects, four diverse functionals with good performance in Table 2—namely, B97-1,²⁷ PW6B95,³² τ -HCTHhyb,⁴⁶ and M06-L¹⁴—were chosen to do tests, with fixed bond lengths, of the importance of relativistic effects. The results of these tests are given in Table 3. The tests involve comparing calculations with the second-order Douglas–Kroll–Hess⁶⁹ scalar relativistic treatment, which is labeled DK in the present article, to calculations with no scalar relativity, which is labeled NDK in the present article. The first B97-1 column is based on a bond length optimized at the same level in the calculations of bond energy as that used for the KS calculations in Table 2. The numbers in all other columns of this table are obtained using the reference bond length given in Table 1; this is denoted by “//ref”. The calculations in Table 3 employ two basis sets: the ma(T)-TZVP basis and a larger basis set that we call apTZ.

The ma(L)-TZVP basis is defined above. Note that the same ma(L)-TZVP basis is used for both NDK and DK calculations.

For the calculations with the larger basis set, we use the notation apTZ to denote a consistent strategy for comparing DK and NDK results. For NDK calculations, apTZ denotes augmented correlation-consistent polarized valence triple- ζ plus outer-core correlation basis set (aug-cc-pwCVTZ-NR)⁷⁰ for transition-metal elements, and nonrelativistic augmented correlation-consistent polarized valence triple- ζ basis set (aug-cc-pVTZ)⁷¹ for ligand elements (H, O, S, and Cl). For scalar relativistic calculations (carried out by the DK method), apTZ denotes using relativistic augmented correlation-consistent polarized valence triple- ζ plus outer-core correlation basis sets (aug-cc-pwCVTZ-DK)⁷⁰ for transition-metal elements, and

relativistic augmented correlation-consistent polarized valence triple- ζ basis set (aug-cc-pVTZ-DK)^{71,72} for other elements.

The smallest MUD(20) in Table 3 is 4.5 kcal/mol for DK calculations by B97-1/apTZ//ref. Furthermore, Table 3 shows that the scalar relativistic effect, on average, weakens the bond⁷³ (i.e., MSD changes by a negative amount), with the MSD(20) difference ranging from -1.8 kcal/mol to -0.6 kcal/mol. However, including scalar relativistic effects changes MUD(20) by only a small amount, between -0.4 kcal/mol and +0.2 kcal/mol. The reason for this is that all NDK values of MSD(20) in Table 3 are positive, i.e., on average all NDK calculations overestimate the bond energies and including scalar relativistic effects is in the correct direction to, on average, reduce the error. (We postpone explanation of the MUD(SR7) and MUD-(MR13) notations in Table 3 until section 7.3.)

Table 4 lists the calculated scalar relativistic effect of the bond energy of each molecule in the 3dMLBE20 database by various methods (including CCSD(T) which will be discussed in a later section), and the mean signed/unsigned relativistic effect (MSRE(20)/MURE(20)) over the 20 bond energies. We can see that the absolute value of relativistic effect ranges from 0.1 kcal/mol to 9.6 kcal/mol. The relativistic effect is especially important for CoCl, CoH, FeH, and CrO, and they all have relativistic effects of >3 kcal/mol for most calculations in Table 4. The various methods in Table 4 usually give similar relativistic effects, except for CoCl and NiCl. The PW6B95/apTZ//ref calculation gives a much smaller relativistic effect for CoCl than do other methods. A small relativistic effect is found for NiCl with B97-1, PW6B95, and τ -HCTHhyb, but large or larger effects are found in M06-L and CCSD(T) calculations.

Table 4 shows that the mean unsigned scalar relativistic effect over 20 bond energies, that is, MURE(20), is in the range of 2.0–2.6 kcal/mol. Hence, the scalar relativistic effect should not be ignored for 3d transition-metal-containing systems. Never-

Table 5. Errors (kcal/mol) of Coupled Cluster, MP2, and DFT Calculations with the ma(L)-TZVP Basis Set^a

		mean signed deviation (except for MUD rows)							
	ROHF	MP2	CCSD	CCSD(T)	CCSDT	CCSDT(2) _Q	B97-1	20xc	MUD(20xc)
3dMLBE-SR7									
MnCl	−5.5	5.8	−3.3	−2.0	−2.2	−2.1	−6.2	−2.7	4.9
ZnCl	−6.8	2.3	−5.8	−4.7	−4.7	−4.6	−5.7	−4.1	4.4
FeCl	−4.8	7.1	−1.6	−0.1	−0.2	−0.1	−1.6	4.5	5.1
CrCl	−33.1	−5.0	−7.8	−5.2	−5.2	−5.1	1.2	−0.2	3.1
ZnS	−36.3	1.4	−10.2	−4.6	−4.8	−4.3	−0.4	−2.8	3.1
ZnH	−3.8	−1.4	−0.3	−0.6	−0.4	−0.4	−2.2	0.0	2.9
CuCl	−27.0	0.6	−6.6	−4.5	−4.5	−4.4	−1.8	−3.1	3.5
MUD(SR7)	16.8	3.4	5.1	3.1	3.2	3.0	2.7	N.A.	3.9
3dMLBE-MR13									
ZnO	−79.3	4.7	−16.9	−7.1	−7.0	−5.9	−8.2	−7.6	7.6
NiCl	−58.1	15.2	−11.4	−6.3	−6.1	−5.9	−0.4	−2.1	2.8
TiCl	−16.0	−2.4	−10.0	−7.9	−7.4	−7.2	−0.3	2.9	3.7
CuH	−32.4	−6.2	−6.1	−4.3	−4.2	−4.1	−1.0	−2.0	2.6
VO	−117.9	2.2	−29.2	−10.8	−11.9	−10.9	−4.6	−6.2	6.8
VCl	−19.7	−4.9	−11.6	−9.6	−9.8	−9.8	−3.0	0.6	2.7
MnS	−60.8	−14.1	−19.5	−12.9	−12.5	−12.4	0.1	−1.6	4.9
CrO	−127.1	−6.9	−26.0	−8.4	−8.4	−7.8	−2.0	−10.4	10.8
CoH	−55.0	5.8	−6.1	−1.7	−0.2	0.3	18.2	14.2	14.3
CoCl	−57.2	7.2	−13.2	−8.3	−7.2	−6.9	12.2	7.6	8.4
VH	−11.2	−4.9	−0.8	−0.5	−0.4	−0.4	7.3	10.6	10.6
FeH	−52.4	−2.4	−4.4	−1.6	−0.5	−0.4	14.7	12.5	12.5
CrH	−27.9	−17.5	−1.5	−0.6	0.1	0.2	7.1	6.2	6.2
MUD(MR13)	55.0	7.3	12.1	6.2	5.8	5.5	6.1	N.A.	7.2
3dMLBE20									
MSD(20)	−41.6	−0.7	−9.6	−5.1	−4.9	−4.6	1.2	0.8	N.A.
MUD(20)	41.6	5.9	9.6	5.1	4.9	4.7	4.9	N.A.	6.0

^aCC calculations in this table are frozen-core NDK/ma(L)-TZVP//ref; B97-1 calculations. Throughout the article, “NDK” denotes noninclusion of scalar relativistic effects; the absence of CV for CC calculations means frozen core; “//ref” means using the bond lengths of Table 1. Errors are always with respect to the reference D_e values; the 20xc and MUD(20xc) columns are the mean signed and unsigned deviations, respectively, averaged over the top 20 xc functional of Table 2, using the consistently optimized bond lengths.

theless, we have seen that the MUD(20) in Table 3 is hardly affected by including scalar relativistic effects, so we expect no significant effect on our conclusions by using the NDK KS calculations in the rest of the article. This is particularly significant for applications since NDK calculations are available in wider range of programs than are DK calculations. Furthermore, Tables 2, 3, and 4 show that our use of the larger apTZ basis set does not markedly decrease the MUD(20) value of calculations with the functionals employed in Tables 3 and 4, and so we will base most of our further discussion of KS accuracy on the more affordable ma(L)-TZVP basis set. Another advantage of the ma(L)-TZVP basis set, as compared to the apTZ set of basis sets, is that ma(L)-TZVP is defined for the entire periodic table of naturally occurring elements, and so it is very convenient for applications.

6. DETAILS OF COUPLED CLUSTER CALCULATIONS

It has been reported that the ROHF reference wave functions usually give substantially better results than spin unrestricted HF (UHF) references,^{7,74} and so we do not test calculations based on unrestricted reference states. However, we do not enforce spin restriction at the CC level; this is sometimes called the RU method (restricted reference, then unrestricted). Within this framework, we carried out the conventional CC calculations at four levels:

- CCSD: single and double excitations in the cluster operator¹

- CCSD(T): single and double excitations in the cluster operator plus quasi-perturbative connected triple excitations³
- CCSDT: single, double, and triple excitations in the cluster operator^{1,50}
- CCSDT(2)_Q: single, double, and triple excitations in the cluster operator with a second-order treatment of connected quadruple excitations⁵¹

All CC calculations are carried out using the fixed bond lengths given in Table 1. The electronic configuration states of the atoms and molecules used in CC calculations also are shown in Table 1.

In most of the CC calculations, we freeze (i.e., do not correlate) all core orbitals of all atoms; in particular, for the first, second, third, and fourth periods, there will be zero, one (1s), five (1s2s2p), and nine (1s2s2p3s3p) frozen orbitals, respectively.

The outer-core–valence (CV) correlation effects of the 3d transition metals and the DK scalar relativistic effects are investigated using the valence-plus-outer-core basis set apTZ at the CCSD(T) level. In the CC calculations correlating outer-core electrons of the 3d transition metals, the outer-core 3s3p orbitals of 3d elements are unfrozen, i.e., only five inner-core orbitals (1s2s2p) of 3d elements are frozen. Considering that the core–valence correlation of the heavy ligand atoms and the inner-core–valence correlation of the 3d metals could also be important, we also correlated all core electrons except for 1s shells of 3d transition metals, S, and Cl at the CCSD(T) level with apwcTZ basis set to calculate the nearly full core–valence

correlation effects (CV'). The notation "apwCvTZ" is used to denote that, in NDK calculations, the aug-cc-pwCvTZ-NR basis set is used for nonhydrogen elements, and aug-cc-pVTZ basis set is used for hydrogen; whereas in DK calculations, it means that the aug-cc-pwCvTZ-DK basis set is used for nonhydrogen elements, and the aug-cc-pVTZ-DK basis set is used for hydrogen.

At the CCSD(T) level, the basis set effect is also tested by comparing the def2-TZVP, ma(L)-TZVP, and ma(L)-TZVPP basis sets, where ma(L)-TZVPP means that the def2-TZVPP⁵⁵ basis set (where PP means heavily polarized) is used for transition-metal elements and hydrogen, and minimally augmented def2-TZVPP basis set (ma-TZVPP) is used for nonhydrogenic ligand elements (L).

All CCSD and CCSD(T) calculations were performed using the Molpro 2010.1 package, and CCSDT and CCSDT(2)_Q were performed using the NWChem 6.3⁷⁵ program. (Note that Molpro and NWChem give identical results at the CCSD and CCSDT levels, but not at the CCSD(T) level, because of additional approximations in the NWChem implementation of the quasi-perturbative triples correction.) In all CC calculations, the basis sets employ spherical-harmonic angular functions.

The CC results and MP2 results are given in Tables 5–10. Notice that an MP2 calculation is carried out by default, along with the CC calculation, when one does a CC calculation with many programs, such as Molpro. The MP2 calculation may be considered to be the first iteration in a full CCSD calculation.⁷⁶

7. DISCUSSION

7.1. KS Performance. On average, the diatomic molecules selected for study here (especially, but not only, CoH) have larger errors (on a per bond basis) than the other molecules in the 3dBE70 database. As explained above, the present study (except in the last two paragraphs of Section 7.4.1 below) shows results for only the 20 xc functionals (out of 42 in the previous study¹⁸) that have the smallest MUD(20) value for the 3dMLBE20 database; these functionals are listed in Table 2. All "errors" are with respect to the reference values in Table 1, and all results used in Table 2 are at consistently optimized geometries, i.e., the geometry is reoptimized with each functional. We can see that, with the ma(L)-TZVP basis set, the top 20 functionals all have MUD(20) < 7.1 kcal/mol, and the top 12 functionals have MUD(20) < 6.0 kcal/mol. The B97-1 functional performs best with an MUD(20) of 5.1 kcal/mol; Table 3 shows that this can be reduced to 4.5 kcal/mol by using a larger basis set.

Because many of the xc functionals have similar average performance on the present database but quite different performance on other databases,^{16,77} the final selection of a functional for study of a particular practical problem should take account of all the available data, including but not limited to the present study.

7.2. Performance of Coupled Cluster Calculations. Although Table 2 is obtained with consistently optimized geometries, it is not usually practical to do optimizations at the CC level. Hence, we use the reference bond lengths given in Table 1 for the CC calculations. Table 3 shows that this is a reasonable strategy when one is considering the mean error over a database. In particular, the second and third columns of Table 3 show that the B97-1 functional has a similar mean unsigned deviation when employed with optimized bond lengths (MUD(20) = 5.1 kcal/mol) and when used with the reference bond lengths of Table 1 (MUD(20) = 4.9 kcal/mol).

Table 5 presents CC and MP2 results with the same ma(L)-TZVP basis set and the same noninclusion of scalar relativistic effects. The CCSD frozen-core calculations have a much larger MUD(20), in particular, 9.6 kcal/mol, than any of the xc functionals listed in Table 2. The CCSD(T) frozen-core calculations reduce the MUD(20) to 5.1 kcal/mol, which is smaller than all but one of the KS results in Table 2. The much-more-expensive full CCSDT calculations and CCSDT(2)_Q calculations further reduce MUD(20) to 4.9 and 4.7 kcal/mol, respectively, which are close to 4.9 kcal/mol of the best functional B97-1 with the same ma(L)-TZVP basis set. By comparing to Table 2, it is concluded that, for NDK calculations with moderate basis set ma(L)-TZVP, frozen core (i.e., uncorrelated 1s2s2p3s3p for 3d transition metals), CCSD(T) perform similarly to a few of the most successful xc functionals, which are much less expensive in computational cost, and CCSDT and CCSDT(2)_Q perform slightly better. We will return to this comparison in section 7.4.

MP2 with the ROHF wave function as reference performs better than CCSD but worse than CCSD(T) for 3dMLBE20, and its MUD(20) is 5.9 kcal/mol with the ma(L)-TZVP basis set, similar to the top 10 xc functionals. However, MP2 is slower in basis set convergence than KS, and later we will see that the MUD(20) of MP2 becomes bigger with a larger basis set apTZ. The two trends mentioned in this paragraph are both well-known from previous work, i.e., MP2 often gives more accurate energies than CCSD and the results often get worse with more complete basis sets. Thus, the MP2 results benefit from recognizable cancellations of errors.

The CC method has also slower basis set convergence than KS, so next we consider Table 6, which shows the effect of basis set on the CCSD(T) calculations, with the sequence of increasing-size basis sets def2-TZVP, ma(L)-TZVP, ma(L)-TZVPP, and apTZ. We can see that, at the same triple- ζ level, using minimally augmented diffuse basis functions for ligand elements (O, S, and Cl), as recommended in ref 56, decreases MUD(20) from 5.9 kcal/mol with def2-TZVP to 5.1 kcal/mol with ma(L)-TZVP, whereas the more heavily polarized ma(L)-TZVPP basis set further decreases the MUD(20) only to 4.9 kcal/mol. The apTZ basis set, which uses aug-cc-pVTZ basis set for H, O, S and Cl and aug-cc-pwCvTZ-NR for transition-metal elements, is a valence plus outer-core correlation basis set, and it significantly decreases the MUD(20) to 3.9 kcal/mol.

Table 7 shows the errors of CC calculations at various excitation levels and MP2 with the apTZ basis set. The table shows that even with this larger basis set, the inclusion of full triples, as in CCSDT, or even full triples and perturbative quadruples, as in CCSDT(2)_Q, yields MUD(20) similar to CCSD(T) for the 3dMLBE20 database; the difference of either of these very expensive sets of calculations from CCSD(T) is only ± 0.1 kcal/mol. MP2 with apTZ basis set has a larger MUD(20) (6.5 kcal/mol) than with ma(L)-TZVP basis set, and it indicates that the smaller MUD(20) with ma(L)-TZVP is due to the cancellation of errors.

The correlation of outer-core 3s and 3p electrons of 3d transition metals is recognized to be important for accurate calculations;⁷⁰ therefore, with the apTZ basis set, we also calculated the outer-core–valence (CV) correlation energy in NDK calculations with CCSD and CCSD(T) and in DK calculations with CCSD(T) by subtracting the energy obtained frozen-core calculations from the energy of calculations in which the outer core orbitals (3s3p) of 3d transition metals are unfrozen. Note that CV correlation lowers the energy for both

Table 6. Error (kcal/mol) of Nonrelativistic Frozen-Core CCSD(T) Calculations with Different Basis Sets Compared to the Reference D_e ^a

	def2-TZVP	ma(L)-TZVP	ma(L)-TZVPP	apTZ
3dMLBE-SR7				
MnCl	−3.8	−2.0	−2.3	−0.6
ZnCl	−4.8	−4.7	−5.3	−4.2
FeCl	−1.9	−0.1	−0.3	1.5
CrCl	−6.2	−5.2	−4.8	−2.9
ZnS	−4.9	−4.6	−5.0	−3.7
ZnH	−0.6	−0.6	1.8	1.2
CuCl	−5.7	−4.5	−4.5	−3.5
MUD(SR7)	4.0	3.1	3.4	2.5
3dMLBE-MR13				
ZnO	−7.7	−7.1	−7.6	−4.6
NiCl	−7.4	−6.3	−2.6	1.1
TiCl	−8.9	−7.9	−7.1	−5.9
CuH	−4.3	−4.3	−0.8	−0.9
VO	−11.7	−10.8	−9.3	−7.0
VCl	−10.7	−9.6	−9.0	−7.2
MnS	−15.0	−12.9	−11.6	−9.0
CrO	−9.9	−8.4	−7.5	−4.9
CoH	−1.7	−1.7	4.1	6.2
CoCl	−9.4	−8.3	−5.3	−1.8
VH	−0.5	−0.5	3.0	3.7
FeH	−1.6	−1.6	3.3	5.4
CrH	−0.6	−0.6	2.1	2.6
MUD(MR13)	6.9	6.2	5.6	4.6
3dMLBE20				
MSD(20)	−5.9	−5.1	−3.4	−1.7
MUD(20)	5.9	5.1	4.9	3.9

^aNDK, frozen core//ref.

the atoms and the molecules so its effect on bond energy, which is shown in Table 8, can have either sign. Table 8 shows that the CV effect is relatively small for molecules containing Cu or Zn, which might have been expected, since these two atoms have a full 3d shell. However, the absolute average of the CV effect over the other 14 diatomics is 1.1–1.3 kcal/mol, so that the average absolute effect for all 20 bond energies (MUCV(20)) in the 3dMLBE20 database is ~0.9–1.0 kcal/mol.

When one correlates more core electrons (2s2p3s3p of 3d transition metals, 2s2p of S and Cl, and 1s of O) in calculations with the apwTZ basis set, the core–valence effect of systems including early transition metals (Ti–Ni) increases by 0.1–0.4 kcal/mol; for molecules containing Cu or Zn, the core–valence effect is decreased by 0–0.3 kcal/mol. As shown in Table 8, when averaged over the 20 molecules in the database, the absolute nearly full core–valence effect (CV') correlating all core electrons except for 1s of 3d transition metals, S, and Cl is 1.1 kcal/mol for NDK and is 1.0 kcal/mol for DK calculations at the CCSD(T) level.

The present work shows that the intershell correlation of outer-core electrons (3s3p) with valence electrons of 3d transition metals and core electrons of heavy atoms, for example 2s2p electrons of S and Cl should not be ignored for high accuracy. However, including only outer-core electrons of 3d transition metals already makes the computational cost extremely high for CCSDT and CCSDT(2)_Q calculations, and even for CCSD(T) calculations it will generally not be affordable for large systems containing 3d transition metals. Table 8 shows that the CV correlation effects have similar trends and

magnitudes at the CCSD and CCSD(T) levels; thus it can be recommended that, when affordable, one adds the CCSD CV effect to CCSD(T) frozen-core calculations. (Similarly, one could add CCSD(T) CV or CV' effects to CCSDT and CCSDT(2)_Q frozen core calculations in those few cases where CCSDT and CCSDT(2)_Q is carried out.)

Tables 9 and 10 compare the errors for a variety of CC with the apTZ or apwTZ basis set and KS calculations with the apTZ basis set. The third row indicates whether a calculation includes scalar relativistic effects (denoted by DK) or not (denoted by NDK). The fourth row indicates whether a CC calculation correlates only valence electrons (denoted V) or also includes outer-core–valence correlation (denoted CV) or nearly full core–valence effect (CV') or is composite.

The composite calculations are CCSD(T), CCSDT, or CCSDT(2)_Q calculations in which outer-core–valence correlation (CV) or nearly full-core–valence effect (CV') and relativistic effects are calculated at a lower level, as motivated by the discussion above. In Table 9, CV(2) denotes that the CV correlation effect obtained in NDK CCSD calculations is added to the frozen-core higher-level calculations; CV(3) denotes that the CV correlation effect obtained by NDK CCSD(T) calculations is added to the frozen-core higher-level calculations; CV(3-DK) denotes that the CV correlation effect obtained by DK calculations at CCSD(T) level is added to the DK frozen-core calculations; and DK(3) denotes that the DK scalar relativistic effect calculated at the CCSD(T) level is added to NDK higher-level calculations. Similarly, in Table 10, CV(3)' denotes that the CV' correlation effect obtained by NDK CCSD(T) calculations is added to the frozen-core higher-level calculations; CV(3-DK)' denotes that the CV' correlation effect obtained by DK calculations at CCSD(T) level is added to the DK frozen-core calculations.

Table 9 shows that the CV(2) correction added to the NDK frozen-core CCSD(T) results gives similar errors to those obtained by direct NDK outer-core-correlated calculations at the CCSD(T) level; MUD(20) increases by 0.2 and 0.1 kcal/mol, respectively, compared to that of the NDK frozen-core calculations, but MSD(20) is improved from −1.7 kcal/mol to −1.2 and −1.3 kcal/mol, respectively. The results are very similar to those obtained in direct CV calculations; this shows that it is a reasonable approximation. Comparison of Tables 9 and 7 also shows that similarly adding the CV(3) to NDK frozen-core CCSDT and CCSDT(2)_Q calculations increases MUD(20) by 0.1–0.2 kcal/mol, but decreases MSD(20) by 0.4–0.5 kcal/mol.

The DK frozen-core calculations at the CCSD(T) level give a MUD(20) of 4.7 kcal/mol, which is 0.8 kcal/mol larger than the NDK value, and this implies that the good performance of NDK CCSD(T) calculations results partly from the cancellation of errors. Adding the CV(3-DK) and DK(3) corrections to NDK frozen-core CCSDT and CCSDT(2)_Q calculations gives MUD(20) = 4.9 and 4.7 kcal/mol, and these values are slightly larger than those for the relativistic calculations (MUD(20) = 4.5 kcal/mol) with B97-1 and the same apTZ basis set. Although the MUD(20) values obtained by composite CCSDT(2)_Q including the CV and scalar relativistic effect calculated at the CCSD(T) level (for convenience, we denote it as CCSDT(2)_Q-CV(3-DK)) and B97-1 DK calculations are approximately similar, their MSD(20) values are quite different, with a difference of 2.9 kcal/mol.

Table 10 shows that using the apwTZ basis set and considering the nearly full core–valence correlation effect (CV') only decrease MUD(20) by 0.1–0.3 kcal/mol at the

Table 7. Error (kcal/mol) of Wave Function Calculations with apTZ Basis Set Compared to the Reference D_e^a

	ROHF	MP2	CCSD	CCSD(T)	CCSDT	CCSDT(2) _Q
3dMLBE-SR6						
MnCl	−3.8	6.0	−1.8	−0.6	−0.7	−0.7
ZnCl	−5.4	1.2	−5.0	−4.2	−4.2	−4.1
FeCl	−3.0	7.2	0.1	1.5	1.5	1.6
CrCl	−31.9	−1.9	−6.0	−2.9	−2.9	−2.8
ZnS	−34.9	1.8	−9.4	−3.7	−3.9	−3.3
ZnH	−3.0	−1.1	1.9	1.2	1.4	1.4
CuCl	−25.8	1.9	−6.0	−3.5	−3.5	−3.4
MUD(SR7)	15.4	3.0	4.3	2.5	2.6	2.5
3dMLBE-MR13						
ZnO	−76.4	8.4	−14.9	−4.6	−4.6	−3.4
NiCl	−57.0	23.0	−5.9	1.1	0.7	0.9
TiCl	−14.9	−1.2	−8.1	−5.9	−5.6	−5.4
CuH	−31.1	−2.2	−3.2	−0.9	−0.9	−0.9
VO	−115.8	5.9	−25.7	−7.0	−8.0	−7.0
VCl	−18.4	−3.8	−9.3	−7.2	−7.4	−7.3
MnS	−58.9	−11.0	−16.3	−9.0	−8.5	−8.4
CrO	−123.9	−2.4	−23.0	−4.9	−4.8	−4.2
CoH	−54.1	14.7	0.3	6.2	6.8	7.2
CoCl	−56.4	14.1	−8.4	−1.8	−1.5	−1.3
VH	−8.7	−1.5	3.5	3.7	3.9	3.9
FeH	−51.7	5.8	0.6	5.4	5.6	5.7
CrH	−25.5	−15.7	1.7	2.6	3.6	3.7
MUD(MR13)	53.3	8.4	9.3	4.6	4.8	4.5
3dMLBE20						
MSD(20)	−40.0	2.5	−6.7	−1.7	−1.6	−1.4
MUD(20)	40.0	6.5	7.5	3.9	4.0	3.8

^aNDK, frozen core//ref.

CCSD(T) level, as compared to results obtained with the apTZ basis set and only considering the outer-core–valence correlation effect (CV) in Table 9. By adding the CV(3-DK)' and DK(3) corrections to the CCSDT(2)_Q results calculated with the apTZ basis set, we got composite CCSDT(2)_Q CV(3-DK)' results. CCSDT(2)_Q CV(3-DK)' has a MUD(20) value of 4.6 kcal/mol, which is similar to that (4.5 kcal/mol) of B97-1 DK calculations, and is only 0.1 kcal/mol better than that of CCSDT(2)_Q CV(3-DK).

7.3. Multireference Diagnostics. On the basis of the above results, with the apTZ basis set, the most complete conventional CC calculations, that is the composite as CCSDT(2)_Q CV(3-DK) or CCSDT(2)_Q CV(3-DK)', and the relativistic calculations using the behaving best xc functional B97-1 have a mean unsigned deviation over 20 bond energies larger than 4.5 kcal/mol. The large error could be due to several reasons, for example, the incomplete basis set used, the uncertainty of the reference experimental bond dissociation energies, or slow convergence with respect to excitation level because of the serious multireference character of many molecules containing transition metals. It is interesting to understand how the extent of multireference character can affect the performance of these methods.

To better understand the extent of multireference character and to learn if there is a diagnostic that will help us to predict the reliability of various types of calculations on new systems, we calculated the three previously proposed multireference diagnostics, which may also be called nondynamical correlation diagnostics. In particular, we calculated the T_1 , M , and B_1 diagnostics. These diagnostics have been reviewed in Section 2, and the results are given in Table 11.

Table 11 shows that the three diagnostics do not agree with each other. The main reason why one calculates diagnostics is the belief that the errors have a tendency to be larger for larger values of the diagnostics, and hence calculating the diagnostic for a new system would provide some guidance, with regard to the reliability of the calculations. One usually expects smaller errors for systems with less multireference character. Hence, we computed the Pearson correlation coefficient (r) between the errors of the composite CCSDT(2)_Q CV(3-DK) or CCSDT(2)_Q CV(3-DK)' calculations and these diagnostics, and we also computed the Pearson correlation coefficients between the diagnostics and relativistic KS calculations with the apTZ basis set. We found insignificant correlations with the unsigned deviations but stronger correlations with the signed deviations. The correlation coefficients with the signed deviations are given in Table 12. We find that the T_1 diagnostics correlate the errors best. Surprisingly, the M diagnostics and B_1 DFT-based diagnostics show weak correlations with the errors.

Because T_1 had the strongest correlations for our database, we used T_1 to divide the 20 molecules in the 3dMLBE20 database into two subsets. The seven molecules, MnCl, ZnCl, FeCl, CrCl, ZnS, ZnH, and CuCl, with $T_1 < 0.03$ are put into a database called 3dMLBE-SR7 with less multireference character (we call it the single reference database, for the sake of convenience), and the other 13 molecules (i.e., those with $T_1 > 0.03$) are assigned to a database called 3dMLBE-MR13 with relatively larger multireference character (we call it the multireference database). The mean unsigned deviations (MUD(SR7)) over the seven bond energies of 3dMLBE-SR7 database and mean unsigned deviations (MUD(MR13)) over the 13 bond energies of

Table 8. Calculated Core–Valence Correlation Energy Effect (kcal/mol) for the 3dMLBE20 Database^a

	Outer-core–valence (CV)			Nearly full core–valence (CV')	
	apTZ			apwcTZ	
	NDK	NDK	DK	NDK	DK
	CCSD	CCSD(T)	CCSD(T)	CCSD(T)	CCSD(T)
TiCl	1.1	0.5	0.3	0.9	0.7
VH	2.2	1.9	1.6	2.1	1.8
VO	1.9	2.9	2.8	3.3	3.1
VCl	1.7	1.2	0.9	1.6	1.3
CrH	0.3	−0.5	−0.6	−0.6	−0.7
CrO	−0.9	−0.2	−0.4	−0.2	−0.3
CrCl	−1.0	−0.7	−1.6	−0.5	−1.5
MnS	0.8	1.1	0.9	1.5	1.3
MnCl	−0.2	−0.7	−0.8	−0.4	−0.5
FeH	1.8	1.6	1.2	1.8	1.4
FeCl	−0.2	−0.5	−0.6	−0.2	−0.3
CoH	2.1	2.1	1.9	2.4	2.1
CoCl	1.8	1.5	1.2	2.0	1.6
NiCl	1.6	1.4	1.2	1.9	1.6
CuH	−0.3	−0.2	−0.2	−0.2	−0.2
CuCl	−0.6	−0.6	−0.7	−0.4	−0.4
ZnH	−0.2	−0.4	−0.4	−0.3	−0.3
ZnO	−0.5	−0.5	−0.5	−0.3	−0.3
ZnS	−0.4	−0.4	−0.4	−0.2	−0.2
ZnCl	−0.4	−0.6	−0.6	−0.3	−0.4
MSCV(20)	0.5	0.4	0.3	0.7	0.5
MUCV(20)	1.0	1.0	0.9	1.1	1.0

^a//ref.

3dMLBE-MR13 are given for various methods in Tables 3, 5, 6, 7, 9, 10, and 13.

Both CC methods and KS density functional methods are single-reference methods, but they both account, to some extent, for static correlations via the introduction of higher-level excitations in CC calculations or by a reasonable choice of exchange functional, since local exchange functionals include some static correlation.^{78,79} It was reported that, for a system with modest multireference character, that the order of accuracy is $\text{CCSD} < \text{CCSD(T)} < \text{CCSDT} < \text{CCSDT(2)}_{\text{Q}}$,⁵¹ and the present study examines whether this performance order is maintained for 3d transition-metal-containing systems with the serious multireference character, in particular, if the order is the same for the single-reference and multireference sub-databases of 3dMLBE20. Inspection of Tables 5, 7, 9, and 10 indicates that, for practical purposes, the three levels, CCSD(T), CCSDT, and CCSDT(2)_Q, have very similar MUD(SR7) values, but the MUD(MR13) value does improve as the higher excitations are included more fully, although CCSDT(2)_Q only slightly improves the accuracy compared to CCSD(T) and CCSDT, except for the NDK frozen-core CC calculations with ma(L)-TZVP basis set for MUD(MR13). The greater effectiveness of higher excitations for multireference cases than for single-reference ones is especially apparent in the MUDs of Table 5.

All tested methods including KS, CC, and MP2 methods have MUD(SR7) smaller than MUD(MR13), as we expected. In all tested methods shown in Tables 3, 5, 6, 7, 9, and 10, if scalar relativistic and core–valence effects are considered, PW6B95/apTZ//ref performs best for less multireference (or single-reference) molecules with an MUD(SR7) of 2.3 kcal/mol (see Tables 3, 9, and 10). The most expensive composite

CCSDT(2)_Q-CV(3-DK)' calculations give MUD(SR7) = 3.7 kcal/mol (see Table 10). CCSD(T) including directly nearly full core–valence effects with the apwcTZ basis set, the composite CCSDT(2)_Q-CV(3-DK)' calculations with the apTZ basis set, and B97-1/apTZ//ref all have the smallest MUD(MR13) value (5.0 kcal/mol) (see Tables 3 and 10). As shown in Tables 7, 9, and 10, the cancellation of errors led to smaller MUD(SR7) and MUD(MR13) values of the CC calculations when the relativistic effect and CV effect are ignored, for example, a MUD(SR7) of 2.5 kcal/mol and a MUD(MR13) of 4.6 kcal/mol can be obtained by NDK frozen core CCSD(T) calculations with the apTZ basis set, and NDK frozen core CCSDT(2)_Q calculations with the apTZ basis set give a MUD(SR7) of 2.5 kcal/mol and a MUD(MR13) of 4.5 kcal/mol, respectively.

Table 13 shows that most NDK calculations of top 20 xc functionals with ma(L)-TZVP perform much better for the single-reference 3dMLBE-SR7 database than for the multi-reference 3dMLBE-MR13 database. Seven functionals have an MUD(SR7) value of <3 kcal/mol, and they are better than or comparable to all NDK frozen-core CC calculations with the same basis set shown in Table 5. The density functionals usually perform worse than CCSD(T) and higher-level CC methods for the multireference 3dMLBE-MR13 database, except for B97-1, which performs similarly to those expensive CC methods.

7.4. Comparison of KS and the CC Calculations.

7.4.1. Absolute Errors. It is well-known that CC calculations have a slower basis set convergence than KS theory, and that is confirmed in the present work. A moderate basis set is often close to convergence for KS theory, but an almost-complete basis set is needed for a well-converged CC calculation, and this requirement adds to the already high cost of CC calculations. Furthermore, whereas core–valence correlation is included by default in DFT, it requires extra work for CC calculations. These considerations of cost lead to the common situation that, in many practical applications of CC theory to complex transition-metal-containing systems, researchers use frozen-core CCSD(T) calculations with a moderate basis set. Therefore, it is very relevant and very interesting that Table 5 shows that NDK frozen-core CCSD(T) calculations, even with a moderate basis set [ma(L)-TZVP], have a MUD(20) value for the 3dMLBE20 database that is 0.9 kcal/mol smaller than the MUD(20) of KS theory when averaged over the top 20 xc functionals (MUD-(20xc)).

However, there is no unique way to answer the question of whether practical conventional CC calculations are more reliable than density functional calculations with currently available functionals. Although we considered more effects (for example, the basis set effect, core–valence effects, relativistic effects, and higher-level excitations in the present work), the practical CC calculations for a moderate realistic system should be NDK frozen-core CCSD(T) calculations with a moderate basis set (for example, ma(L)-TZVP). If we consider the best performing density functional, namely B97-1, Table 5 shows that, when ignore the scalar relativistic effect, for the same ma(L)-TZVP basis set, its mean unsigned deviation is smaller than that of CCSD(T), the same as that of CCSDT, and almost as small as that of CCSDT(2)_Q. One must also interpret the results in light of the finite size and diversity of the basis set and possible experimental errors in the reference data. The mean unsigned deviation of 5.1 kcal/mol for CCSD(T) has a standard deviation of 3.8 kcal/mol. Thus, all 20 xc functionals in Table 1 have MUDs well within one standard deviation of that for CCSD(T), and 19

Table 9. Error (kcal/mol) of Coupled Cluster Calculations and DFT Calculations with the apTZ Basis Set Compared to the Reference D_e^a

	Direct			Composite ^b						Direct	
	CCSD(T)	CCSD(T)	CCSD(T)	CCSD(T)	CCSD(T)	CCSDT	CCSDT	CCSDT(2) _Q	CCSDT(2) _Q	B97-1	PW6B95
	NDK	NDK	DK	DK	NDK	NDK	DK(3)	NDK	DK(3)	DK	DK
	V	CV	V	CV	CV(2)	CV(3)	CV(3-DK)	CV(3)	CV(3-DK)		
3dMLBE-SR7											
MnCl	−0.6	−1.3	−2.1	−2.9	−0.8	−1.4	−3.1	−1.4	−3.0	−7.3	0.4
ZnCl	−4.2	−4.9	−7.1	−7.8	−4.6	−4.8	−7.7	−4.7	−7.6	−7.3	−5.5
FeCl	1.5	1.0	−0.6	−1.2	1.4	1.0	−1.2	1.0	−1.1	−3.2	2.1
CrCl	−2.9	−3.6	−3.8	−5.4	−3.9	−3.6	−5.4	−3.5	−5.3	2.2	−2.2
ZnS	−3.7	−4.1	−5.8	−6.2	−4.1	−4.3	−6.4	−3.7	−5.9	−1.5	−2.9
ZnH	1.2	0.8	−0.2	−0.6	0.9	1.1	−0.3	1.1	−0.3	−2.8	0.0
CuCl	−3.5	−4.1	−3.6	−4.2	−4.0	−4.2	−4.3	−4.1	−4.2	−0.5	−3.2
MUD(SR7)	2.5	2.8	3.3	4.1	2.8	2.9	4.1	2.8	3.9	3.5	2.3
3dMLBE-MR13											
ZnO	−4.6	−5.1	−7.3	−7.7	−5.1	−5.0	−7.7	−3.8	−6.5	−8.0	−10.9
NiCl	1.1	2.5	−7.1	−6.0	2.7	2.1	−6.3	2.2	−6.2	−0.8	−2.6
TiCl	−5.9	−5.4	−7.2	−7.0	−4.9	−5.1	−6.6	−4.9	−6.5	−1.9	3.1
CuH	−0.9	−1.1	1.7	1.5	−1.2	−1.1	1.5	−1.0	1.5	2.7	1.2
VO	−7.0	−4.0	−7.5	−4.8	−5.1	−5.0	−5.8	−4.0	−4.8	−4.2	−2.8
VCl	−7.2	−6.1	−9.0	−8.1	−5.5	−6.2	−8.3	−6.1	−8.2	−4.8	1.1
MnS	−9.0	−7.8	−10.5	−9.6	−8.2	−7.3	−9.1	−7.3	−9.0	−1.6	−0.1
CrO	−4.9	−5.1	−0.9	−1.3	−5.9	−5.0	−1.1	−4.4	−0.5	2.9	−6.6
CoH	6.2	8.4	1.9	3.8	8.4	8.9	4.4	9.3	4.8	11.2	16.8
CoCl	−1.8	−0.3	−8.1	−6.9	0.0	0.0	−6.7	0.2	−6.5	3.4	7.9
VH	3.7	5.6	2.1	3.7	5.9	5.8	3.9	5.8	3.9	6.1	12.7
FeH	5.4	6.9	2.5	3.7	7.2	7.2	4.0	7.3	4.1	9.2	11.0
CrH	2.6	2.1	4.2	3.6	2.9	3.1	4.6	3.2	4.7	9.0	5.5
MUD(MR13)	4.6	4.6	5.4	5.2	4.8	4.8	5.4	4.6	5.2	5.0	6.3
3dMLBE20											
MSD(20)	−1.7	−1.3	−3.4	−3.2	−1.2	−1.2	−3.1	−0.9	−2.8	0.1	1.3
MUD(20)	3.9	4.0	4.7	4.8	4.1	4.1	4.9	4.0	4.7	4.5	4.9

^a//ref. ^bSee text (Section 7.2).

of them even have MUD values within one-half of a standard deviation of CCSD(T).

Table 5 shows that B97-1 has a smaller MUD value than CCSD(T) both for single-reference systems and for multi-reference ones. Furthermore, even when the results are averaged over the top 20 functionals, the improvement by CCSD(T) over KS theory is about the same for the single-reference system as for the multi-reference system; in particular, Table 5 shows that the MUD(SR7) of CCSD(T) is lower than the average MUD(SR7) of the top 20 xc functionals by 0.8 kcal/mol, and the MUD(MR13) of CCSD(T) is lower than the average MUD(MR13) of the top 20 xc functionals by 1.0 kcal/mol.

Another question we can ask is this: even though KS theory performs almost as well as CCSD(T) in an average sense, are there particular molecules for which all KS calculations are much worse than CCSD(T)? Table 14 presents results relevant to this question. The column labeled “top 20” functionals shows, for each molecule, how many of them have errors smaller than those of CCSD(T). Although most of this paper considers just the 20 best functionals (those in Table 2), for a moment, it is interesting to consider the full set of all 42 functionals of ref 18, and the last column of Table 14 shows how many of these have errors smaller than that of CCSD(T) for each molecule. When we consider the top 20 functionals, on average, 9 of them perform better than CCSD(T) for a given single-reference molecule, and 10 of them perform better than CCSD(T) for a given multi-reference

molecule. Even when we consider the full set of 42 functionals, on average, 16 of the 42 perform better than CCSD(T) for single-reference cases, and, on average, 18 of the 42 perform better than CCSD(T) for multi-reference cases. The choice of xc functional for a given problem may be dependent on many factors, but these results show that, even for a wide group of functionals, the KS calculation often yields more-accurate results than CCSD(T).

Some of the cases in Table 14 merit further discussion. The only molecule for which CCSD(T) has a smaller error than all 42 xc functionals is FeH; for this case, the best performing functional is M06-2X, with an absolute error that is 0.8 kcal/mol larger than that of CCSD(T). There are four cases where only one xc functional has an absolute error smaller than that of CCSD(T); those cases and the identity of the best performing functional are as follows: FeCl (M06-2X), CoH (M06-2X), VH (M05-2X), and CrH (SOGGA11). For ZnH, only M08-SO, MPWLYP1M, and B1LYP have absolute errors smaller than those of CCSD(T). In the other 14 cases, at least 8 and as many as 34 functionals (out of the 42 tested) perform better than CCSD(T).

7.4.2. Signed Errors. Usually CCSD(T) calculations underestimate the bond energies, but KS-DFT broken-symmetry calculations overestimate the bond energies. This difference in the signs is a serious problem and can lead to incorrect inferences when one compares KS theory to CCSD(T) theory. For example, even if we use the data obtained by the most complete

Table 10. Error (kcal/mol) of Coupled Cluster Calculations and DFT Calculations Compared to the Reference D_e^a

	Direct/apwcTZ				Composite ^b /apTZ				Direct/apTZ	
	CCSD(T)	CCSD(T)	CCSD(T)	CCSD(T)	CCSDT	CCSDT	CCSDT(2) _Q	CCSDT(2) _Q	B97-1	PW6B95
	NDK	NDK	DK	DK	NDK	DK(3)	NDK	DK(3)	DK	DK
	V	CV'	V	CV'	CV(3)'	CV(3-DK)'	CV(3)'	CV(3-DK)'		
3dMLBE-SR7										
MnCl	−0.5	−0.9	−2.0	−2.6	−1.2	−2.8	−1.1	−2.7	−7.3	0.4
ZnCl	−4.1	−4.4	−7.0	−7.3	−4.5	−7.5	−4.4	−7.3	−7.3	−5.5
FeCl	1.6	1.4	−0.4	−0.8	1.3	−0.9	1.3	−0.8	−3.2	2.1
CrCl	−2.8	−3.2	−3.7	−5.2	−3.4	−5.4	−3.2	−5.2	2.2	−2.2
ZnS	−3.4	−3.6	−5.5	−5.7	−4.1	−6.2	−3.5	−5.7	−1.5	−2.9
ZnH	1.2	0.9	−0.2	−0.5	1.1	−0.2	1.1	−0.2	−2.8	0.0
CuCl	−3.2	−3.6	−3.3	−3.8	−3.9	−4.1	−3.8	−4.0	−0.5	−3.2
MUD(SR7)	2.4	2.6	3.2	3.7	2.8	3.9	2.7	3.7	3.5	2.3
3dMLBE-MR13										
ZnO	−4.5	−4.9	−7.2	−7.5	−4.9	−7.6	−3.7	−6.4	−8.0	−10.9
NiCl	1.4	3.2	−6.9	−5.2	2.6	−5.9	2.7	−5.7	−0.8	−2.6
TiCl	−5.8	−5.0	−7.2	−6.5	−4.7	−6.3	−4.5	−6.1	−1.9	3.1
CuH	−0.9	−1.1	1.7	1.5	−1.1	1.5	−1.0	1.6	2.7	1.2
VO	−7.1	−3.7	−7.6	−4.5	−4.6	−5.4	−3.7	−4.4	−4.2	−2.8
VCl	−7.1	−5.5	−8.9	−7.6	−5.8	−7.9	−5.7	−7.8	−4.8	1.1
MnS	−8.6	−7.1	−10.1	−8.8	−7.0	−8.7	−6.9	−8.6	−1.6	−0.1
CrO	−4.9	−5.0	−0.9	−1.2	−4.9	−1.1	−4.3	−0.5	2.9	−6.6
CoH	6.2	8.6	1.9	4.0	9.2	4.6	9.6	5.0	11.2	16.8
CoCl	−1.5	0.4	−7.9	−6.3	0.5	−6.2	0.7	−6.0	3.4	7.9
VH	3.7	5.8	2.1	3.9	6.0	4.1	6.0	4.1	6.1	12.7
FeH	5.4	7.2	2.5	3.9	7.4	4.2	7.5	4.3	9.2	11.0
CrH	2.6	2.0	4.2	3.5	3.0	4.5	3.1	4.6	9.0	5.5
MUD(MR13)	4.6	4.6	5.3	5.0	4.7	5.2	4.6	5.0	5.0	6.3
3dMLBE20										
MSD(20)	−1.6	−0.9	−3.3	−2.8	−0.9	−2.9	−0.7	−2.6	0.1	1.3
MUD(20)	3.8	3.9	4.6	4.5	4.1	4.8	3.9	4.6	4.5	4.9

^a//ref. ^bSee text (Section 7.2).

Table 11. Multireference Diagnostics

	T_1	M	B_1
MnCl	0.016	0.011	4.3
ZnCl	0.017	0.016	−1.6
FeCl	0.021	0.007	10.5
CrCl	0.022	0.030	2.9
ZnS	0.023	0.137	4.7
ZnH	0.025	0.028	−1.3
CuCl	0.027	0.016	1.8
ZnO	0.036	0.344	15.4
NiCl	0.038	0.017	4.1
TiCl	0.038	0.106	6.9
CuH	0.039	0.043	4.7
VO	0.053	0.174	30.7
VCl	0.057	0.011	6.7
MnS	0.057	0.179	21.3
CrO	0.066	0.234	27.9
CoH	0.067	1.041	3.3
CoCl	0.068	1.172	3.3
VH	0.095	0.026	5.8
FeH	0.111	0.714	6.9
CrH	0.146	0.063	3.4

composite, CCSDT(2)_Q-CV(3-DK)' results as the benchmark for the 3dMLBE20 database to validate B97-1 DK calculations using the same basis set; we will get a mean unsigned difference of 4 kcal/mol, but the two methods actually have the similar

Table 12. Pearson Correlation Coefficients r between the Errors of Composite Relativistic Core–Valence CCSDT(2)_Q Calculations and Relativistic KS-DFT Calculations with apTZ Basis Set

	Pearson correlation coefficient, r		
	T_1	M	B_1
CCSDT(2) _Q -CV(3-DK)'	0.60	0.22	−0.15
CCSDT(2) _Q -CV(3-DK)	0.59	0.20	−0.15
B97-1	0.74	0.50	−0.14
PW6B95	0.57	0.53	−0.31
τ -HCTHhyb	0.75	0.59	−0.05
M06-L	0.60	0.38	0.01

performance against the experimental results. It could be even more serious for a specific system (e.g., for the bond energy of VCl) if we were to use the result of CCSDT(2)_Q-CV(3-DK)' as a benchmark, the errors of relativistic B97-1 and PW6B95 would be inferred to be 3.0 and 8.9 kcal/mol, respectively; however, with the experimental reference, the real errors of two methods are −4.8 and 1.1 kcal/mol. Thus, using CC theory as a benchmark would lead to a totally wrong conclusion for PW6B95 (unless the experimental results are wrong).

7.5. Uncertainties of the Reference Data. All the conclusions we obtained above are based on the available experimental reference data (bond lengths and D_e) shown in Table 1. The surprising large MUD(20) of the conventional

Table 13. Exchange–Correlation Functionals Tested in This Work and Their Mean Unsigned Deviations (MUD(SR7)) over 7 Bond Energies of the 3dMLBE-SR7 Sub-database and Mean Unsigned Deviations (MUD(MR13)) over the 13 Bond Energies of the 3dMLBE-MR13 Sub-database, Compared to the Reference D_e Values Given in Table 1^a

xc	MUD(SR7) (kcal/mol)	MUD(MR13) (kcal/mol)	xc	MUD(SR7) (kcal/mol)	MUD(MR13) (kcal/mol)
B97-1	3.2	6.1	MPWB1K	2.1	8.0
ω B97X-D	2.7	6.9	M08-HX	2.4	7.9
MPW1B95	2.5	7.1	B3LYP	5.2	6.6
PW6B95	2.8	7.0	PBE0	2.9	7.9
PW6B95-D3(BJ)	3.2	6.9	M06	6.3	6.6
τ -HCTHhyb	4.1	6.6	M06-2X	3.6	8.3
M06-D3(BJ)	5.8	5.7	ω B97X	4.5	8.0
B97-3	3.2	7.2	O3LYP	3.8	8.4
M08-SO	2.0	7.9	HSE	6.3	7.2
M06-L	3.2	7.4	M05	7.6	6.8

^aThis table is based on calculations including spin–orbit coupling, but neglecting scalar relativistic effects (which is denoted NDK). It is based on consistently optimized bond lengths (i.e., bond lengths for each xc functional optimized with that functional), and the ma(L)-TZVP basis set is used for all results in this table.

Table 14. Number of Functionals That Have a Error Smaller Than That of NDK Frozen-Core CCSD(T) Calculations with the ma(L)-TZVP Basis Set for Each Molecule

	top 20 functionals	42 functionals
	3dMLBE-SR7	
MnCl	6	8
ZnCl	11	20
FeCl	1	1
CrCl	17	30
ZnS	14	26
ZnH	1	3
CuCl	15	24
average	9	16
	3dMLBE-MR13	
ZnO	8	18
NiCl	18	34
TiCl	17	27
CuH	17	34
VO	15	20
VCl	20	33
MnS	19	26
CrO	8	18
CoH	1	1
CoCl	10	19
VH	0	1
FeH	0	0
CrH	0	1
average	10	18

single-reference CC methods for the 3dMLBE20 database were found even when we considered the both vector (spin–orbit coupling) and scalar relativistic effects (DK), nearly full core–valence effect (CV'), and higher excitation up to quadruples. This makes one suspect the accuracy of experiments.

Previous experience, the first two columns of Table 3, and additional tests not presented here, indicate to us that if the bond lengths used in the D_e calculations are reasonable, they will have a small effect on the averaged error. Thus, we can ignore the effect of the uncertainties of bond lengths used in the calculations.

The stated uncertainties of the reference experimental D_e are listed in Table 1, and they are 0.4–2 kcal/mol. If we apply the largest uncertainty (2 kcal/mol) to all the reference data leading

to the MUD(20) and assume that the experimental error in every case makes the deviation from the CC calculation large (an extremely unlikely scenario), the error in the most complete composite CCSDT(2)_Q-CV(3-DK)/apTZ results would decrease to MUD(20) = 2.6 kcal/mol and NDK frozen-core CCSD(T)/ma(L)-TZVP results would decrease to MUD(20) = 3.1 kcal/mol. However, similarly, there is the possibility that the MUD(20) of the xc functional also decreases by a comparable amount. Using the CC method as a reference favors the xc functionals that have the same signed deviations as the CC methods, and it would overestimate the errors of the xc functionals that have the oppositely signed deviations from the correct results. From this point of view, we suggest that one still must be cautious to take the practical CC calculations as a reference to validate or compare various xc functionals.

8. SUMMARY

The present comparisons of theory with experiment do not justify using practical conventional single-reference CC calculations as a benchmark for Kohn–Sham (KS) calculations, since these CC calculations deviate more than density functional results when compared to available experimental data. In the present work, we constructed a new database called 3dMLBE20, which consists of 20 reference equilibrium bond energies of 3d transition-metal-containing diatomic molecules that are obtained from experimental heats of formation or experimental bond dissociation energies. The 3dMLBE20 database is divided into two subsets. One is called 3dMLBE-SR7 and includes seven molecules with lesser amounts of multireference character in their wave functions; the other is 3dMLBE-MR13, and it includes 13 molecules with relatively larger multireference character. The CC methods tested include conventional CCSD, CCSD(T), CCSDT, and CCSDT(2)_Q; the results for the 3dMLBE20 database and its subsets are compared with the results of KS density functional calculations.

As part of the process, the DKH scalar relativistic effect and outer-core–valence correlation (CV) effects on the bond energy of 3d transition-metal–ligand bond energies are investigated. The absolute average of the scalar relativistic effect and core–valence effect over the 20 bonds in the 3dMLBE20 database are ~ 2 –3 kcal/mol and ~ 1 kcal/mol, respectively. For some individual molecule, the scalar relativistic effect can be as large as ~ 9 kcal/mol, and the core–valence effect can be up to 3 kcal/

mol, so that neither of the two effects can be ignored in the investigation of similar systems.

In all of our comparisons, we include vector relativistic effects (spin–orbit coupling) in the calculated bond energies by both CC and KS methods.

With a relatively large basis set, apwTZ, when both scalar relativistic and nearly full core–valence correlation effects (CV') are considered, CCSD(T) gives a mean unsigned deviation over the 20 bond energies of the 3dMLBE20 database (MUD(20)) of 4.5 kcal/mol. The more-expensive full CCSDT and CCSDT(2)_Q do not improve the performance remarkably, and they change the MUD(20) values to 4.8 and 4.6 kcal/mol, respectively. These performances are better than we obtain with most xc functionals, but a good xc functional with the slightly smaller apTZ basis set—for example, B97-1 (MUD(20) = 4.5 kcal/mol), or PW6B95 (MUD(20) = 4.9 kcal/mol)—can give similar and even slightly closer-to-experiment results. The CC calculations neglecting quadruple excitations, scalar relativistic effects, and core–valence correlation and with a quasi-perturbative treatment of connected triple excitations have a smaller MUD(20) value, in particular 3.8–4.0 kcal/mol, but looking at the trends of all results shows that this is partly because of the cancellation of errors.

We found that both CC calculations and KS density functional calculations perform better for the single-reference subset (3dMLBE-SR7) than the multireference subset (3dMLBE-MR13). PW6B95/apTZ//ref calculations including scalar relativistic effects perform best for 3dMLBE-SR7 with an MUD(SR7) value of 2.3 kcal/mol. For this subset, the relativistic nearly full core–valence correlation CCSD(T)/apwTZ, and the composite CCSDT, and CCSDT(2)_Q calculations with the apTZ basis set by adding the DK effect and CV' calculated at CCSD(T) level to the corresponding frozen-core results have a MUD(SR7) value of ~3.7–3.9 kcal/mol.

All CC and KS density functional methods have MUD-(MR13) values larger than 4.5 kcal/mol.

The CC methods tested here are usually impractically expensive for applications to most problems in transition-metal chemistry. However, even if they were affordable or when they become affordable, conventional CC methods including CCSD(T), CCSDT, and CCSDT(2)_Q have performance (judged by comparison to available experimental data) only comparable to, but not necessarily better than KS density functional calculations with a wide set of choices of xc functionals, and they cannot be assumed to provide validated benchmarks for KS theory. Of course, it is possible that one would draw different conclusions if the experimental data were found to be inaccurate.

AUTHOR INFORMATION

Corresponding Author

*E-mail: truhlar@umn.edu.

Notes

The authors declare no competing financial interest.

ACKNOWLEDGMENTS

The authors are grateful to Karol Kowalski, Piotr Piecuch, So Hirata, and Jingjing Zheng for helpful discussions and correspondence. This work was supported in part by the U.S. Department of Energy, Office of Basic Energy Sciences, Division of Chemical Sciences, Geosciences, and Biosciences, under Award No. DE-FG02-12ER16362. This research was performed in part using the computing resources of the MSCF in EMSL, a

national scientific user facility sponsored by the U.S. DOE, Office of Basic Energy Research and located at PNNL.

REFERENCES

- (1) (a) Cizek, J. *J. Chem. Phys.* **1966**, *45*, 4256. (b) Lee, T. J.; Scuseria, G. E. In *Quantum Mechanical Electronic Structure Calculations with Chemical Accuracy*; Langhoff, S. R., Ed.; Understanding Chemical Reactivity, Vol. 13; Kluwer Academic Publishers: Dordrecht, The Netherlands, 1995; p 47. (c) Cramer, C. J. *Essentials of Computational Chemistry*; John Wiley & Sons: Chichester, U.K., 2002; p 191. (d) Bartlett, R. J.; Musial, M. *Rev. Mod. Phys.* **2007**, *79*, 291. (e) Shavitt, I.; Bartlett, R. J. *Many-Body Methods in Chemistry and Physics: MBPT and Coupled-Cluster Theory*; Cambridge University Press: Cambridge, U.K., 2009.
- (2) (a) Schütz, M.; Werner, H.-J. *Chem. Phys. Lett.* **2000**, *318*, 370. (b) Schütz, M.; Werner, H.-J. *J. Chem. Phys.* **2001**, *114*, 661. (c) Fedorov, D. G.; Kitaura, K. *J. Chem. Phys.* **2005**, *123*, 134103. (d) Kobayashi, M.; Nakai, H. *J. Chem. Phys.* **2008**, *129*, 044103. (e) Li, W.; Piecuch, P. *J. Phys. Chem. A* **2010**, *114*, 8644. (f) Werner, H.-J.; Schütz, M. *J. Chem. Phys.* **2011**, *135*, 144116. (g) Anacker, T.; Friedrich, J. *Mol. Phys.* **2013**, *111*, 1161. (h) Friedrich, J.; Yu, H.; Leverentz, H. R.; Bai, P.; Siepmann, J. I.; Truhlar, D. G. *J. Phys. Chem. Lett.* **2014**, *5*, 666. (i) Fiedler, L.; Leverentz, H. R.; Nachimuthu, S.; Friedrich, J.; Truhlar, D. G. *J. Chem. Theory Comput.* **2014**, *10*, 3129.
- (3) Raghavachari, K.; Trucks, G. W.; Pople, J. A.; Head-Gordon, M. *Chem. Phys. Lett.* **1989**, *157*, 479.
- (4) (a) Kinal, A.; Piecuch, P. *J. Phys. Chem. A* **2006**, *110*, 367. (b) Valeev, E. F.; Crawford, T. D. *J. Chem. Phys.* **2008**, *128*, 244113. (c) Czako, G.; Mátyus, E.; Simmonett, A. C.; Császár, A. G.; Schaefer, H. F., III; Allen, W. D. *J. Chem. Theory Comput.* **2008**, *4*, 1220. (d) Rahalkar, A. P.; Mishra, B. K.; Ramanathan, V.; Gadre, S. R. *Theor. Chem. Acc.* **2011**, *130*, 491. (e) Liakos, D. G.; Neese, F. *J. Phys. Chem. A* **2012**, *116*, 4801. (f) Booth, G. H.; Grüneis, A.; Kresse, G.; Alavi, A. *Nature* **2013**, *493*, 365.
- (5) (a) Kohn, W.; Sham, L. J. *Phys. Rev.* **1965**, *140*, A1133. (b) Kohn, W. *Rev. Mod. Phys.* **1999**, *71*, 1253.
- (6) Werner, H.-J.; Knowles, P. J.; Knizia, G.; Manby, F. R.; Schütz, M. *Wiley Interdiscip. Rev.: Comput. Mol. Sci.* **2012**, *2*, 242.
- (7) Jiang, W.; DeYonker, N. J.; Determan, J. J.; Wilson, A. K. *J. Phys. Chem. A* **2011**, *116*, 870.
- (8) Martin, J. M. L. *Mol. Phys.* **2014**, *112*, 785.
- (9) (a) Andersson, K.; Malmqvist, R.-Å.; Roos, B. O.; Sadlej, A. J.; Wolinski, K. *J. Phys. Chem.* **1990**, *94*, 5483. (b) Andersson, K.; Malmqvist, R.-Å.; Roos, B. O. *J. Chem. Phys.* **1992**, *96*, 1218.
- (10) (a) Van Voorhis, T.; Head-Gordon, M. *J. Chem. Phys.* **2000**, *113*, 8873. (b) Bishop, R. F.; Arponen, J. S. *Int. J. Quantum Chem., Quantum Chem. Symp.* **1990**, *38*, 197. (c) Van Voorhis, T.; Head-Gordon, M. *Chem. Phys. Lett.* **2000**, *330*, 585. (d) Piecuch, P.; Oliphant, N.; Adamowicz, L. *J. Chem. Phys.* **1993**, *99*, 1875. (e) Li, X. Z.; Paldus, J. J. *J. Chem. Phys.* **1997**, *107*, 6257. (f) Li, X. Z.; Paldus, J. J. *J. Chem. Phys.* **1998**, *108*, 637. (g) Krylov, A. I.; Ssherrill, C. D.; Byrd, E. F. C.; Head-Gordon, M. *J. Chem. Phys.* **1998**, *109*, 10669. (h) Hino, O.; Kinoshita, T.; Chan, G. K. L.; Bartlett, R. J. *J. Chem. Phys.* **2006**, *124*, 114311. (i) Nooijen, M.; Bartlett, R. J. *J. Chem. Phys.* **1997**, *107*, 6812. (j) Levchenko, S. V.; Krylov, A. I. *J. Chem. Phys.* **2004**, *120*, 175. (k) Kowalski, K.; Piecuch, P. *J. Chem. Phys.* **2000**, *113*, 18. (l) Lodriguito, M. S.; Kowalski, K.; Wloch, M.; Piecuch, P. *J. Mol. Struct.* **2006**, *771*, 89. (m) Evangelista, F. A.; Simmonett, A. C.; Allen, W. D.; Schaefer, H. F., III; Gauss, J. *J. Chem. Phys.* **2008**, *128*, 124104.
- (11) (a) DeYonker, N. J.; Peterson, K. A.; Steyl, G.; Wilson, A. K.; Cundari, T. R. *J. Phys. Chem. A* **2007**, *111*, 11269. (b) Karlický, F.; Otyepka, M. *J. Chem. Theory Comput.* **2011**, *7*, 2876. (c) Seth, M.; Ziegler, T.; Steinmetz, M.; Grimme, S. *J. Chem. Theory Comput.* **2013**, *9*, 2286. (d) Karlický, F.; Lazar, P.; Dubecký, M.; Otyepka, M. *J. Chem. Theory Comput.* **2013**, *9*, 3670.
- (12) Engel, E.; Dreizler, R. M. *Density Functional Theory*; Springer: Berlin, 2011.
- (13) Schuch, N.; Verstraete, S. *Nat. Phys.* **2009**, *5*, 732.
- (14) Zhao, Y.; Truhlar, D. G. *J. Chem. Phys.* **2006**, *125*, 194101.

- (15) Zhao, Y.; Truhlar, D. *Theor. Chem. Acc.* **2008**, *120*, 215.
- (16) (a) Cramer, C. J.; Truhlar, D. G. *Phys. Chem. Chem. Phys.* **2009**, *11*, 10757. (b) Peverati, R.; Truhlar, D. G. *Philos. Trans. R. Soc. A* **2014**, *372*, 20120476.
- (17) Zhang, W.; Truhlar, D. G.; Tang, M. J. *Chem. Theory Comput.* **2014**, *10*, 2399.
- (18) Zhang, W.; Truhlar, D. G.; Tang, M. J. *Chem. Theory Comput.* **2013**, *9*, 3965.
- (19) Perdew, J. P.; Ruzsinszky, A.; Csonka, G. I.; Constantin, L. A.; Sun, J. *Phys. Rev. Lett.* **2009**, *103*, 026403.
- (20) Staroverov, V. N.; Scuseria, G. E.; Tao, J.; Perdew, J. P. *J. Chem. Phys.* **2003**, *119*, 12129.
- (21) Grimme, S.; Antony, J.; Ehrlich, S.; Krieg, H. *J. Chem. Phys.* **2010**, *132*, 154104.
- (22) Grimme, S.; Ehrlich, S.; Goerigk, L. *J. Comput. Chem.* **2011**, *32*, 1456.
- (23) Peverati, R.; Truhlar, D. G. *Phys. Chem. Chem. Phys.* **2012**, *14*, 13171.
- (24) Zhao, Y.; Schultz, N. E.; Truhlar, D. G. *J. Chem. Phys.* **2005**, *123*, 161103.
- (25) Hoe, W.-M.; Cohen, A. J.; Handy, N. C. *Chem. Phys. Lett.* **2001**, *341*, 319.
- (26) Becke, A. D. *Phys. Rev. A* **1988**, *38*, 3098.
- (27) Hamprecht, F. A.; Cohen, A. J.; Tozer, D. J.; Handy, N. C. *J. Chem. Phys.* **1998**, *109*, 6264.
- (28) Perdew, J. P.; Burke, K.; Ernzerhof, M. *Phys. Rev. Lett.* **1996**, *77*, 3865.
- (29) Stephens, P. J.; Devlin, F. J.; Chabalowski, C. F.; Frisch, M. J. *J. Phys. Chem.* **1994**, *98*, 11623.
- (30) Zhao, Y.; Truhlar, D. G. *J. Phys. Chem. A* **2004**, *108*, 6908.
- (31) Peverati, R.; Truhlar, D. G. *J. Chem. Theory Comput.* **2012**, *8*, 2310.
- (32) Zhao, Y.; Truhlar, D. G. *J. Phys. Chem. A* **2005**, *109*, 5656.
- (33) Zhao, Y.; Truhlar, D. G. *J. Chem. Phys.* **2008**, *128*, 184109.
- (34) Heyd, J.; Scuseria, G. E.; Ernzerhof, M. *J. Chem. Phys.* **2003**, *118*, 8207.
- (35) Henderson, T. M.; Izmaylov, A. F.; Scalmani, G.; Scuseria, G. E. *J. Chem. Phys.* **2009**, *131*, 044108.
- (36) Adamo, C.; Barone, V. *J. Chem. Phys.* **1999**, *110*, 6158.
- (37) Keal, T. W.; Tozer, D. J. *J. Chem. Phys.* **2005**, *123*, 121103.
- (38) Peverati, R.; Truhlar, D. G. *Phys. Chem. Chem. Phys.* **2012**, *14*, 16187.
- (39) Chai, J.-D.; Head-Gordon, M. *Phys. Chem. Chem. Phys.* **2008**, *10*, 6615.
- (40) Zhao, Y.; Truhlar, D. G. *J. Chem. Theory Comput.* **2008**, *4*, 1849.
- (41) Peverati, R.; Truhlar, D. G. *J. Chem. Phys.* **2011**, *135*, 191102.
- (42) Zhao, Y.; Schultz, N. E.; Truhlar, D. G. *J. Chem. Theory Comput.* **2006**, *2*, 364.
- (43) Peverati, R.; Truhlar, D. G. *J. Phys. Chem. Lett.* **2011**, *2*, 2810.
- (44) Adamo, C.; Barone, V. *Chem. Phys. Lett.* **1997**, *274*, 242.
- (45) Chai, J.-D.; Head-Gordon, M. *J. Chem. Phys.* **2008**, *128*, 084106.
- (46) Boese, A. D.; Handy, N. C. *J. Chem. Phys.* **2002**, *116*, 9559.
- (47) (a) Peverati, R.; Truhlar, D. G. *J. Phys. Chem. Lett.* **2012**, *3*, 117. (b) Peverati, R.; Zhao, Y.; Truhlar, D. G. *J. Phys. Chem. Lett.* **2011**, *2*, 1991.
- (48) Gáspár, R. *Acta Phys. Hung.* **1974**, *35*, 213.
- (49) Vosko, S. H.; Wilk, L.; Nusair, M. *Can. J. Phys.* **1980**, *58*, 1200.
- (50) (a) Noga, J.; Bartlett, R. J. *J. Chem. Phys.* **1987**, *86*, 7041. (b) Scuseria, G. E.; Schaefer, H. F., III. *Chem. Phys. Lett.* **1988**, *152*, 382. (c) Watts, J. D.; Bartlett, R. J. *J. Chem. Phys.* **1990**, *93*, 6104.
- (51) Hirata, S.; Fan, P. D.; Auer, A. A.; Nooijen, M.; Piecuch, P. J. *Chem. Phys.* **2004**, *121*, 12197.
- (52) Rinaldo, D.; Tian, L.; Harvey, J. N.; Friesner, R. A. *J. Chem. Phys.* **2008**, *129*, 164108.
- (53) (a) Möller, C.; Plesset, M. S. *Phys. Rev.* **1934**, *46*, 618. (2) Martin, H.-G.; Pople, J. A.; Frisch, M. J. *Chem. Phys. Lett.* **1988**, *153*, 503.
- (54) Armentrout, P. B.; Kickel, B. L. In *Organometallic Ion Chemistry*; Frieser, B. S., Ed.; Understanding Chemical Reactivity, Vol. 15; Kluwer Academic Publishers: Dordrecht, The Netherlands, 1996; p 1.
- (55) Weigend, F.; Ahlrichs, R. *Phys. Chem. Chem. Phys.* **2005**, *7*, 3297.
- (56) Zheng, J.; Xu, X.; Truhlar, D. *Theor. Chem. Acc.* **2011**, *128*, 295.
- (57) (a) Lee, T. J.; Taylor, P. R. *Int. J. Quant. Chem. Symp.* **1989**, *S23*, 199. (b) Lee, T. J.; Rice, J. E.; Scuseria, G. E.; Schaefer, H. F. *Theor. Chim. Acta* **1989**, *75*, 81.
- (58) Jiang, W.; DeYonker, N. J.; Wilson, A. K. *J. Chem. Theory Comput.* **2012**, *8*, 460.
- (59) Tishchenko, O.; Zheng, J.; Truhlar, D. G. *J. Chem. Theory Comput.* **2008**, *4*, 1208.
- (60) Werner, H.-J.; Knowles, P. J. *J. Chem. Phys.* **1985**, *82*, 5053.
- (61) Knowles, P. J.; Werner, H.-J. *Chem. Phys. Lett.* **1985**, *115*, 259.
- (62) Schultz, N. E.; Zhao, Y.; Truhlar, D. G. *J. Phys. Chem. A* **2005**, *109*, 11127.
- (63) Cook, M.; Karplus, M. *J. Phys. Chem.* **1987**, *91*, 31.
- (64) Fogueri, U. R.; Kozuch, S.; Karton, A.; Martin, J. M. L. *Theor. Chem. Acc.* **2013**, *132*, 1291.
- (65) Wernel, H.-J.; Knowles, P. J.; Knizia, G.; Manby, F. R.; Schütz, M.; Celani, P.; Korona, T.; Lindh, R.; Mitrushenkov, A.; Rauhut, G.; Shamasundar, K. R.; Adler, T. B.; Amos, R. D.; Bernhardsson, A.; Berning, A.; Cooper, D. L.; Deegan, M. J. O.; Dobbyn, A. J.; Eckert, F.; Goll, E.; Hampel, C.; Hesselmann, A.; Hetzer, G.; Hrenar, T.; Jansen, G.; Köppl, C.; Liu, Y.; Lloyd, A. W.; Mata, R. A.; May, A. J.; McNicholas, S. J.; Meyer, W.; Mura, M. E.; Nicklass, A.; O'Neill, D. P.; Palmieri, P.; Pflüger, K.; Pitzer, R.; Reiher, M.; Shiozaki, T.; Stoll, H.; Stone, A. J.; Tarroni, R.; Thorsteinsson, T.; Wang, M.; Wolf, A. *Molpro, version 2010.1, A Package of Ab Initio Programs*; available via the Internet at: <http://www.molpro.net>.
- (66) Berning, A.; Schweizer, M.; Werner, H.-J.; Knowles, P. J.; Palmieri, P. *Mol. Phys.* **2000**, *98*, 1823.
- (67) (a) Frisch, M. J.; Trucks, G. W.; Schlegel, H. B.; Scuseria, G. E.; Robb, M. A.; Cheeseman, J. R.; Scalmani, G.; Barone, V.; Mennucci, B.; Petersson, G. A.; Nakatsuji, H.; Caricato, M.; Li, X.; Hratchian, H. P.; Izmaylov, A. F.; Bloino, J.; Zheng, G.; Sonnenberg, J. L.; Hada, M.; Ehara, M.; Toyota, K.; Fukuda, R.; Hasegawa, J.; Ishida, M.; Nakajima, T.; Honda, Y.; Kitao, O.; Nakai, H.; Vreven, T.; Montgomery, J. A., Jr.; Peralta, J. E.; Ogliaro, F.; Bearpark, M.; Heyd, J. J.; Brothers, E.; Kudin, K. N.; Staroverov, V. N.; Keith, T.; Kobayashi, R.; Normand, J.; Raghavachari, K.; Rendell, A.; Burant, J. C.; Iyengar, S. S.; Tomasi, J.; Cossi, M.; Rega, N.; Millam, J. M.; Klene, M.; Knox, J. E.; Cross, J. B.; Bakken, V.; Adamo, C.; Jaramillo, J.; Gomperts, R.; Stratmann, R. E.; Yazyev, O.; Austin, A. J.; Cammi, R.; Pomelli, C.; Ochterski, J. W.; Martin, R. L.; Morokuma, K.; Zakrzewski, V. G.; Voth, G. A.; Salvador, P.; Dannenberg, J. J.; Dapprich, S.; Daniels, A. D.; Farkas, O.; Foresman, J. B.; Ortiz, J. V.; Cioslowski, J.; Fox, D. J. *Gaussian 09, Revision C.01*; Gaussian, Inc.: Wallingford, CT, 2010. (b) Zhao, Y.; Peverati, R.; Yang, K.; Truhlar, D. G. *Minnesota Density Functionals Module 6.4, MN-GFM 6.4*. See <http://comp.chem.umn.edu/mn-gfm/> for details.
- (68) Xu, X.; Truhlar, D. G. *J. Chem. Theory Comput.* **2012**, *8*, 80.
- (69) (a) Douglas, M.; Kroll, N. M. *Ann. Phys. (N.Y.)* **1974**, *82*, 89. (b) Jansen, G.; Hess, B. A. *Phys. Rev. A* **1989**, *39*, 6016.
- (70) Balabanov, N. B.; Peterson, K. A. *J. Chem. Phys.* **2005**, *123*, 064107.
- (71) (a) Dunning, T. H., Jr. *J. Chem. Phys.* **1989**, *90*, 1007. (b) Kendall, R. A.; Dunning, T. H., Jr.; Harrison, R. J. *J. Chem. Phys.* **1992**, *96*, 6796. (c) Woon, D. E.; Dunning, T. H., Jr. *J. Chem. Phys.* **1993**, *98*, 1358.
- (72) de Jong, W. A.; Harrison, R. J.; Dixon, D. A. *J. Chem. Phys.* **2001**, *114*, 48.
- (73) Hess, B. A. *Relativistic Effects in Heavy-Element Chemistry and Physics*; Wiley: Chichester, U.K., 2003.
- (74) Williams, T. G.; DeYonker, N. J.; Ho, B. S.; Wilson, A. K. *Chem. Phys. Lett.* **2011**, *504*, 88.
- (75) Valiev, M.; Bylaska, E. J.; Govind, N.; Kowalski, K.; Straatsma, T. P.; van Dam, H. J. J.; Wang, D.; Nieplocha, J.; Apra, E.; Windus, T. L.; de Jong, W. A. *Comput. Phys. Commun.* **2010**, *181*, 1477.
- (76) Adams, G. F.; Bent, G. D.; Bartlett, R. J.; Purvis, G. D. In *Potential Energy Surfaces and Dynamics Calculations*; Truhlar, D. G., Ed.; Plenum Press: New York, 1979; p 133.
- (77) (a) Valdes, H.; Pluháčková, K.; Pitonák, M.; Řezáč, J.; Hobza, P. *Phys. Chem. Chem. Phys.* **2008**, *10*, 2747. (b) Korth, M.; Grimme, S. *J. Chem. Theory Comput.* **2009**, *5*, 993. (c) Tekarli, S. M.; Drummond, M.

- L.; Williams, T. G.; Cundari, T. R.; Wilson, A. K. *J. Phys. Chem. A* **2009**, *113*, 8607. (d) Goerigk, L.; Grimme, S. *Phys. Chem. Chem. Phys.* **2011**, *13*, 6670. (e) Elm, J.; Bilde, M.; Mikkelsen, K. V. *J. Chem. Theory Comput.* **2012**, *8*, 2071.
- (78) Gritsenko, O. V.; Schipper, P. R. T.; Baerends, E. J. *J. Chem. Phys.* **1997**, *107*, 5007.
- (79) Handy, N. C.; Cohen, A. J. *Mol. Phys.* **2001**, *99*, 403.
- (80) Yungman, V. S. *Thermal Constants of Substances*, Vol. 5; John Wiley & Sons: New York, 1999.
- (81) Chase, J. M. W.; Davies, C. A.; Downey, J. J. R. Frurip, D. J.; McDonald, R. A.; Syverud, A. N. NIST-JANAF Tables. *J. Phys. Chem. Ref. Data, Monogr.* **1998**, *9*, 1.
- (82) Kardahakis, S.; Mavridis, A. *J. Phys. Chem. A* **2009**, *113*, 6818.
- (83) Jensen, K. P.; Roos, B. O.; Ryde, U. *J. Chem. Phys.* **2007**, *126*, 014103.
- (84) Harrison, J. F. *Chem. Rev.* **2000**, *100*, 679.
- (85) Bach, R. D.; Shobe, D. S.; Schlegel, H. B.; Nagel, C. J. *J. Phys. Chem.* **1996**, *100*, 8770.